TURUN YLIOPISTO

Petrography and genesis of Vaajasalmi graphite targets in Rautalampi, Central Finland

Jaakko Nurkkala

Geologia
pro gradu -tutkielma
Laajuus: 30 op

Ohjaajat:
Esa Heilimo
Janne Kuusela

21.10.2022
Turku

Master's thesis

Subject: Geology
Author: Jaakko Nurkkala
Title: Petrography and genesis of Vaajasalmi graphite targets in Rautalampi, Central Finland
Supervisors: Esa Heilimo & Janne Kuusela
Number of pages: 56 pages
Date: 21.10.2022

Abstract

Natural graphite is listed on the European Union's top 30 most critical minerals and is mainly imported outside of Europe. Graphite value and demand increase are driven by electrification since its extraordinary features in the conductance of electricity and heat. The Geological Survey of Finland has done wide studies on graphite in recent years and they believe the qualities of the bedrock and metamorphic grade in Finland are suitable for economically potential graphite deposits.

This thesis study mineralogy and the genesis of Vaajasalmi area graphite targets in Rautalampi municipality in Central Finland. The two flake graphite targets were first discovered by the Geological Survey of Finland during the battery mineral exploration campaign. The petrographic study was conducted from 16 thin sections with polarization and reflected light microscopes. Genesis and quality of the graphite and metamorphic degree of the rocks were determined by scanning electron microscope (SEM), Raman spectroscopy, petrography. Further, the thesis solves Vaajasalmi graphite targets mineralogical properties, the difference between targets, genesis and formation temperature of the graphite.

The graphite has remobilized and enriched via deformation-driven intensive shearing that also produces higher purity of graphite. Comparison to average Finnish Svecofennian sediments pseudosections gives an estimate of high amphibole facies conditions in the study area with temperatures ranging from 650 to 750 °C and pressure from 5 to 9.5 kbar. Impurities inside the graphite are derived from the surrounding minerals and the best quality graphite is associated with recrystallized-looking quartz clusters.

Key words: Graphite, Rautalampi, Central- Finland, Raman, Geothermometer, Scanning Electron Microscopy, Petrography

Table of contents

1 Introduction 5

2 Graphite 7

2.1 Properties of graphite 7

2.2 Graphite deposits in Finland 8

3 Geological background 11

3.1 Svecofennian geology 12

3.2 Rautalampi local geology 14

4 Materials and methods 18

4.1 Petrographic analysis from thin sections 18

4.2 Scanning electron microscope and backscatter electron-images 18

4.3 Raman spectroscopy 19

4.3.1 Theory of Raman spectroscopy 20

5 Results 23

5.1 General petrographic description 23

5.2 Detail petrographic description and division based on types of graphite 25

5.2.1 Detailed petrography of type 1 graphite samples 25

5.2.2 Detailed petrography of type 2 graphite samples 26

5.2.3 Detailed petrography of type 3 graphite samples 28

5.2.4 Detailed petrography of types 4 and 5 graphite samples 30

5.3 SEM-EDS results 31

5.4 Whole-rock analysis and drillhole profiles 33

5.5 Raman spectroscopy and geothermometer 36

6 Discussion 39

6.1 Comparison between targets 39

6.2 Raman analysis and geothermometer 40

6.3 Regional P/T- estimation 41

6.4 Graphite genesis 45

7 Conclusion 50

Acknowledgements **51**

References **52**

Appendices **55**

1 Introduction

Graphite is the most common carbon allotrope in the Earth's crust, it is formed from layers of pure carbon (C). Approximately half of the Worlds graphite reserves are hosted by China. Mozambique and Tanzania also host significant reserves, each with a 15% share. Within the EU, the largest natural graphite deposits are located in Sweden, Czech Republic and Finland (European Commission 2020). Only 2% of the EU consumption of natural graphite is produced inside the EU, mainly in the Germany and Austria. Natural graphite is imported to the EU principally from China, which provides 47% of the EU demand. Other main suppliers are Brazil (12%), Norway (8%) and Zimbabwe (7%). China is the largest producer and exporter of natural graphite in 2017 with market shares of 71 % and 59 %. Consumption of natural graphite is related to steel production, due to its use in refractories. The most recent use and need for the supply of natural graphite is the development of electric vehicles and energy storage systems, batteries. The European Union (EU) has included graphite in the list of critical minerals since 2010. An updated version of the list was published in September 2020 with natural graphite in it. Materials on the critical mineral list are selected based on the risks of supply and high economic impact on the EU. Previous development is seen to drive most of the growth in the future natural graphite demand (European Commission 2020).

Graphite can be divided into synthetic- and natural graphite based on the production. Synthetic graphite is made from hydrocarbons like coal coke, petroleum and coal. Natural graphite occurs in three different forms classified by purity and particle size: microcrystalline, vein-type and crystalline flake type. microcrystalline graphite is the most common type, but its quality is the lowest of these three. Flake-type graphite is the most important form for commercial use. Finland is considered to be potential for new flake graphite deposit discoveries according to the Geological Survey of Finland (GTK). Flake graphite is commonly located in high metamorphic grade paragneiss, schists and mica-rich quartzites, all qualities found in Finnish bedrock. (Ahtola & Kuusela, 2015)

The aim of this study is to determine the mineralogy of the Vaajasalmi graphite targets found in Rautalampi municipality in Central Finland (Fig. 1). The methods used in this thesis are microscopy, scanning electron microscope (SEM), carbon whole rock analysis, and Raman spectroscopy. The thesis aims to solve Vaajasalmi graphite mineralogical properties, the difference between targets, genesis and formation temperature of the graphite.

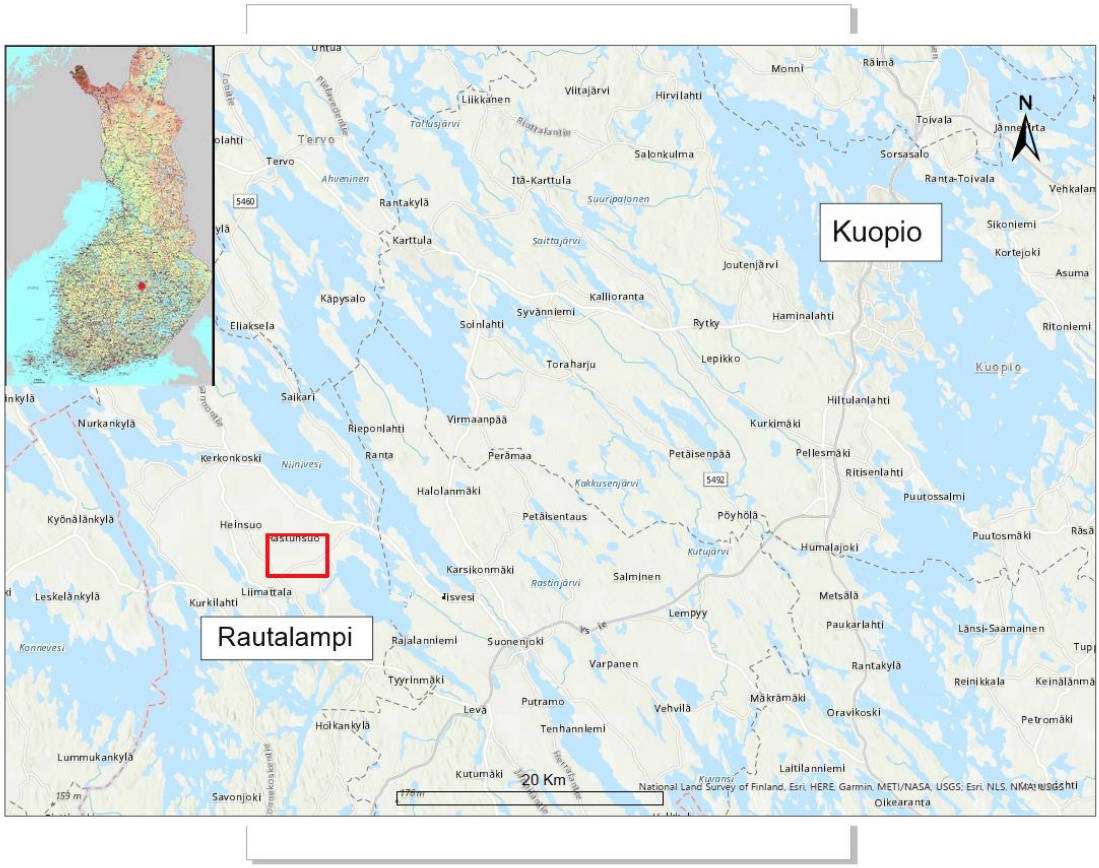

Figure 1. Location of the Vaajasalmi study area, marked by a red rectangle (Kuusela et al., 2021)

2 Graphite

2.1 Properties of graphite

Carbon is the 15th most abundant element in the Earth's crust. The atoms of carbon can bond in different ways and form four individual allotropes: 1) carbon nanotube, 2) diamond, 3) fullerenes and 4) graphite (Fig. 2). The most common allotrope of solid carbon is graphite, characterized by grey-black color, metallic luster, soft appearance 1-2 on Mohs scale and low density 2.09-2.23g/cm^3 (Simandi et al. 2015). Graphite has a layered structure where carbon atoms are bonded with covalent bonds in hexagonal arrays (Fig. 2). These single layers are called graphene layers. Graphene layers are connected by Van der Waals interactions to create a weak secondary bond. These weak bonds between the layers result in low shear strength, slippery feel and clear cleavage. Structure makes each layer of graphite a good thermal and electrical conductor along the sheets, but not perpendicular to it. (Ahtola & Kuusela, 2015, Simandl et al., 2015)

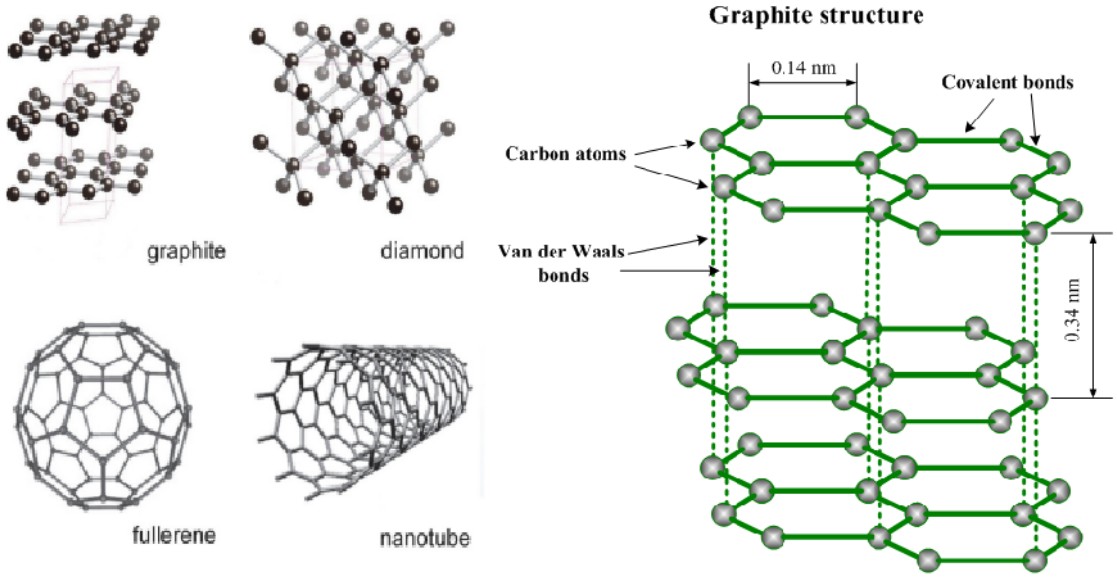

Figure 2. Structures of allotropes of carbon and more detailed picture of graphite structure. (Oganov, 2013)

Economically interesting natural graphites occur in three main types: 1) microcrystalline (amorphous), 2) vein graphite and 3) crystalline flake graphite. Economically significant graphite deposits are presumably formed by either maturation of organic material with later

metamorphism or by the precipitation of graphite from C-H-O-fluids (metamorphic or metasomatic) (Simandl et al., 2015). Microcrystalline graphite is regarded as the most common and cheapest type of graphite. It is commonly used as a lubricant due to physical properties like fine grain-size and low reflectance. Microcrystalline graphite deposits are typically formed in contact metamorphism with low-greenschist to greenschist facies conditions or in regional metamorphism of coal seams (Simandl et al., 2015).

The vein-type deposits are regarded as the most significant from the economical perspective, due to the exceptionally high quality of the graphite. Typically, the vein graphite is found in metasedimentary units with upper amphibolite or granulite facies metamorphism. These deposits are found in or in the vicinity of igneous intrusions, in skarn-type assemblages. (Simandl et al., 2015)

Crystalline flake graphite is found disseminated in various rocks including paragneisses, quartzites, pegmatites, marbles, iron formations, and syenites. The most common host for economically notable deposits is paragneiss or marble which has been subjected to metamorphism in upper amphibolite or granulite facies. Thick paragneiss sequences commonly host evenly mineralized graphite deposits with a general grade of 2-3 % graphite. Typical high-grade graphite deposits are along or near marble-paragneiss contacts or in the crests of folds accompanied by epidote and chlorite as retrograde minerals. Enrichment of graphite may probably be the result of two different setups; 1) decreasing temperature of C-O-H-fluids or 2) decarbonation-reactions in marbles and dehydration-reactions in paragneiss produce a mixture of fluids. The fluids could also be derived from pegmatites or other minor intrusions. (Simandl et al. 2015) Graphite deposits in Finland

2.2 Graphite deposits in Finland

Black schists are the most common host rock for the graphite deposits in Finland. By definition black schists are originally deposited on the seabed and it contains at least 1% of organic carbon and sulphur each (Lehtinen et al. 1998). The black schists are relatively common in eastern and northern Finland. These supracrustal rocks are deposited in anaerobic conditions and then metamorphosed black shales are aged c. 2.06-1.85 Ga. All bedrock observations with mention of flake graphite from GTK and Outokumpu Oy databases are presented on the map in Figure 3. It also contains drillhole observations with mentions of flake graphite and map layer of known black schists in Finland. Different graphite targets have been identified practically in all schist and migmatite belts in Finland. Targets consisting

of flake graphite are not that numerous and locate in regions with metamorphic degree higher than middle-amphibolite facies. This makes the areas with carbon-containing schists and the high metamorphic degree to be considered as potential for flake graphite. This would highlight the regions like granulite facies areas of Uusimaa and Saimaa schist belt, migmatite area of Pirkkala, SW-edge of Lapland granulite belt and its nearby migmatite areas (Fig. 3). (Ahtola & Kuusela 2015)

Laitakari (1925) published a comprehensive study listing about 120 graphite targets mainly in southern and eastern Finland. According to Puustinen (2003) graphite has been produced in Finland in 30 deposits from 1760 to 1947 and 10 of those are now located on the Russian side of the border. From the remaining 20 deposits, 14kt ore was mined and 10kt of it was mined from Kärpälä, Mäntyharju, South-Savo. which was mined with 39% ore grade of graphite. These deposits are currently or contemporary considered as minor or insignificant lenses, but still offers relevant information and signs for potential flake graphite deposits (Ahtola & Kuusela, 2015).

The latest major exploration for graphite in Finland was conducted by GTK in the beginning of 1980s after the energy crisis. Emphasis of the study was to locate and research economically potential deposits with geological and geophysical exploration methods (Ahtola & Kuusela 2015). The most interesting deposits were microcrystalline graphite occurrences in Kiihtelysvaara (Sarapää et al. 1984a) and in Juuka (Sarapää et al.1984b), Northern Savo. The most potential regions were selected and these included Peräpohja schist belt, Central-Lapland schist belt and Tampere schist belt, (Ahtola & Kuusela 2015; Fig. 5). Deposits in the report consist of two different sections: 1) “old deposits” with earlier mining activity with clearly flake type graphite. Potential areas for flake graphite were identified in Kärpälä and Piippumäki (Palosaari et al. 2020) in Mäntyharju municipality South Savo, Ala-Heimari and Laasolanmäki in Ristiina area, North Karelia , minor graphite targets in Vammala, Pirkanmaa region and Haapamäki deposit in Leppävirta, North Savo, which has been recently studied by Nygård (2017), Puronaho (2018), and Eriksson (2018). 2) “Other deposits” which consist of black shale areas with typically graphite with finer flake size but locally occurring coarse flaked lenses. Like in most of the studies also the study of Nurmela (1989) highlight the importance of the high metamorphic degree in graphite deposits.

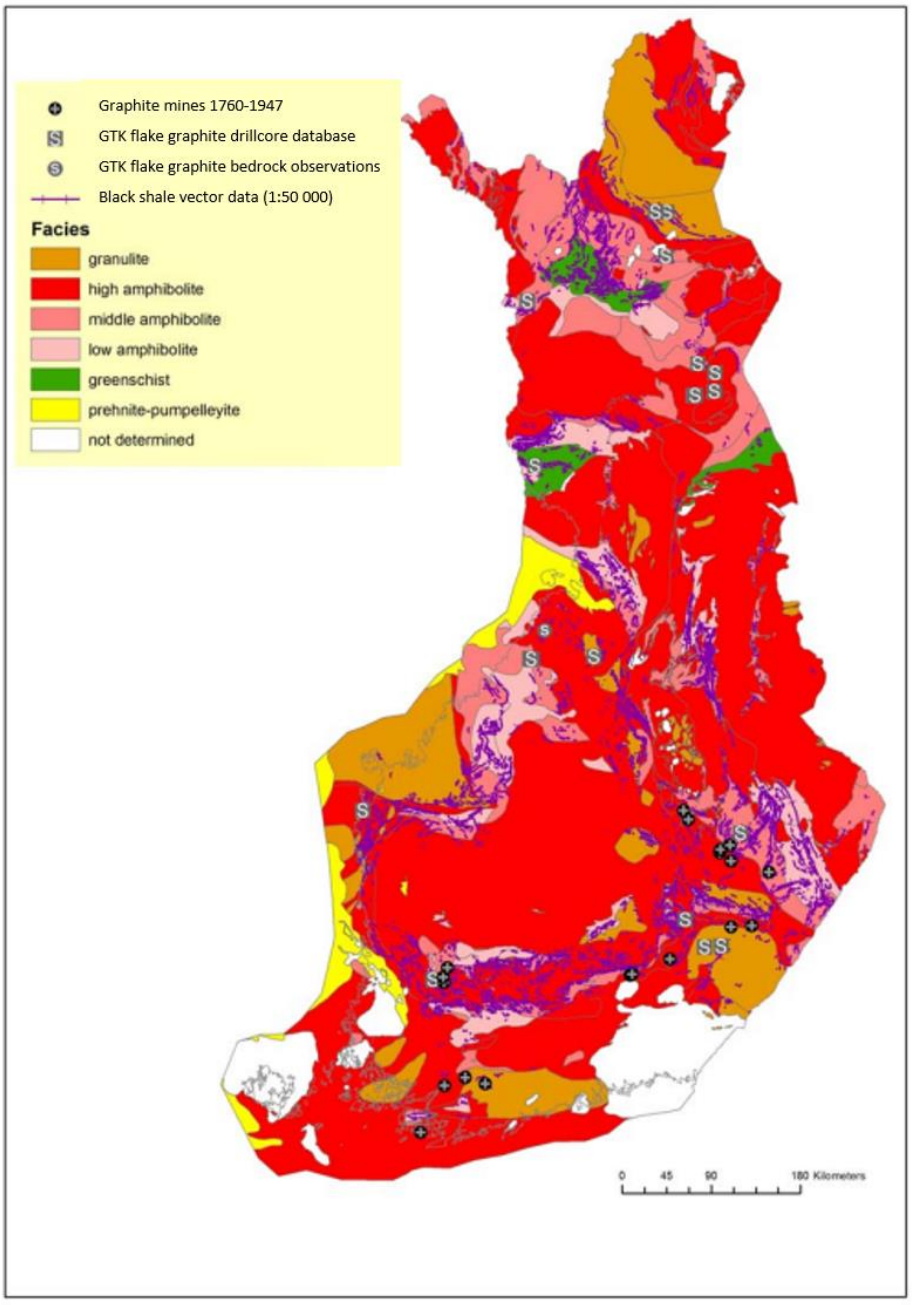

Figure 3. Map of flake graphite targets and black schist areas collected from GTK-databases and presented on a metamorphic map of Finland 1:1000000 (Ahtola & Kuusela, 2015)

3 Geological background

The bedrock of Finland is part of Precambrian Fennoscandian shield that formed via amalgamation of four major tectonic provinces; Karelia, Lapland- Kola, Norrbotten and Svecofennia (Fig. 4; Nironen, 2017). The eastern and northern parts of Finland are a part of Karelia, Lapland-Kola and Norrbotten provinces that contain of Archean bedrocks (3.5-2.5 Ga; Mutanen & Huhma, 2003, Nironen, 2017). The first fundamental Paleoproterozoic event in the evolution of Fennoscandia shield was the break-up of the initial Archean continent occurred 2.44-2.05 Ga that broke the Karelia, Lapland-Kola and Norrbotten provinces. The second event was mainly convergent Svecofennian orogeny at 1.92-1.77 Ga (Nironen, 2017). Paleoproterozoic Svecofennian rocks in the southern- and central-part of Finland are mainly aged 1.93-1.8 Ga. Only a minor portion of Finnish bedrock is younger than 1.77 Ga (Kähkönen, 1998). The Rapakivi batholiths formed 1.65-1.54 Ga are considered the last major bedrock formation in Finland (Nironen, 2017). The southern Finland anorthosites and mafic dyke swarms are associated with Rapakivi batholiths. The other young rocks are sedimentary rocks in southwestern Finland and accretionary bedrock in northwestern Finland during the Phanerorozoic Caledonides orogeny.

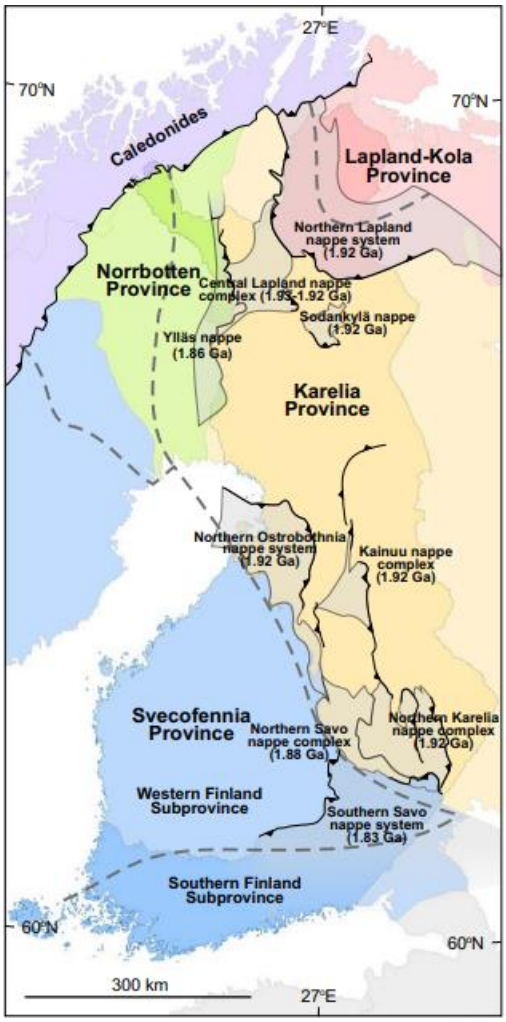

Figure 4. Lithological units and tectonic boundaries in Finland. (Nironen 2017)

3.1 Svecofennian geology

The Svecofennian supracrustal bedrock is abundant of metasediments with differing metamorphic overprints (Fig. 5). Supracrustal lithologies vary from phyllites, mica schists, mica gneisses to migmatites. Granitic intrusives and mafic metavolcanites, associated to island arc volcanism, are most typical rocks in Svecofennian bedrock. In between of the metasediments, different types of volcanites are present as own schist belts and interlayers. In paragneisses and metapelitic rocks, the black schists are typically present as narrow interlayers and lenses especially in eastern Finland (Kähkönen, 1998). The peak of metamorphic grade in the Svecofennian province is from the upper amphibolite facies to granulite facies at pressures between 4-6 kbar and temperatures varying from 700 ºC to 880 ºC (Hölttä & Heilimo 2017).

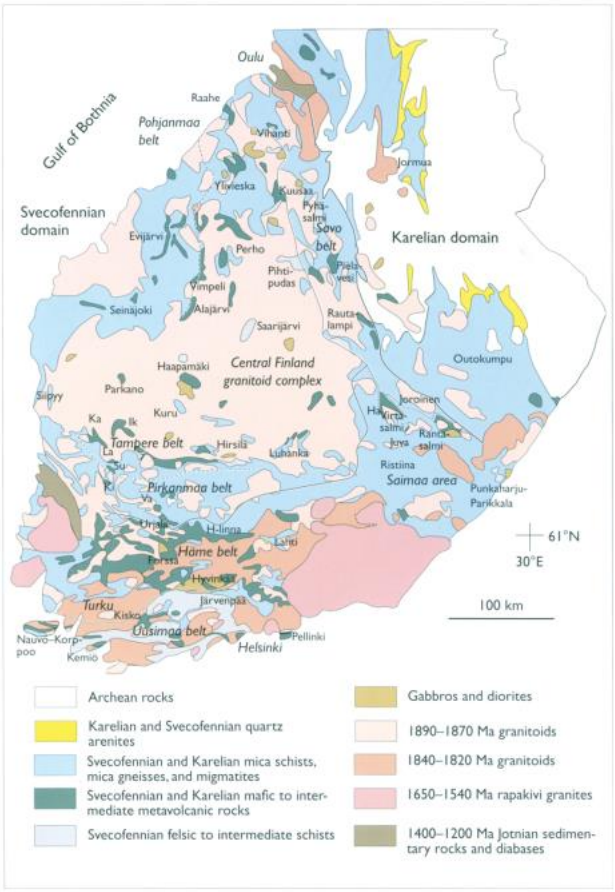

Figure 5. Simplified geological map of Southern and Central Finland (Kähkönen, 2005).

The study area is located in the Savo schist belt which is bordered with Central Finland Granitoid complex in the west and with Karelia schist belt and archean craton in the northeast. Majority of the rocks of Svecofennia are aged to 1.905-1.880 Ga, but the rocks of Savo schist belt are moderately older, 1.93-1.92 Ga. Typical foliation in Savo schist belt rocks is NNW-SSE oriented. The rocks are typically strongly migmatized and metamorphosed in upper amphibole to granulite facies. The Savo schist belt is controlled by various fault zones especially in the margins of tectonic settings with Archean province and Karelian schist belt in the NE and Saimaa schist belt in the S). Due to intensive faulting, the majority of the rocks are strongly sheared and the belt consist of differing blocks. (Kähkönen, 1998)

In terms of dominant lithologies Savo schist belt contains typical turbiditic mica schists, gneisses and migmatites are the most common in the Savo schist belt. Metavolcanites are common interlayers in few areas, for example in the Rautalampi area. Black schists and graphite-bearing schists are frequent in the Savo schist belt. Sedimentary carbonates, cordierite-antophyllite-(garnet)-gneisses and volcanogenic massive sulphide deposits are

locally found from the unit. These sulphide deposits have been mined for example in the middle of Savo schist belt at Pyhäsalmi and Vihanti (Fig. 5; Kähkönen 1998).

3.2 Rautalampi local geology

Study area Vaajasalmi is located in Central Finland, approximately 60 km to southwest from Kuopio in Rautalampi municipality (Fig. 1). The Rautalampi area is affected by Raahe-Laatokka- fracture zone, East from the study area. Bedrock of the Rautalampi consists mainly from early Proterozoic synorogenic granitoids; granites, granodiorites, tonalites and monzonitic rocks. Among the igneous rocks there are remnants of supracrustic formations, metapelites and metavolcanites (Figs. 6, 7). Metamorphism took place in upper amphibolite facies conditions and locally in granulite facies (Pääjärvi, 2000). According to metamorphic map of Finland by Hölttä & Heilimo (2017) the study area has metamorphosed under granulite facies conditions (Fig. 8). Age of the rocks is estimated to extend from 1.93 to 1.91 Ga (Lahtinen, 1994). Various fractures and faults are typical cutting features in bedrock (Pääjärvi, 2000). In the East Vaajasalmi area is bordered with NE-SW- trending Iisvesi fault (Fig. 6; Koistinen & Vihreäpuu 1982) and major transpressional fault separates Vaajasalmi from the nearby Käpysuo area (Fig. 6; Kuusela et al., 2021) suggesting the study area to be affected with numerous faults.

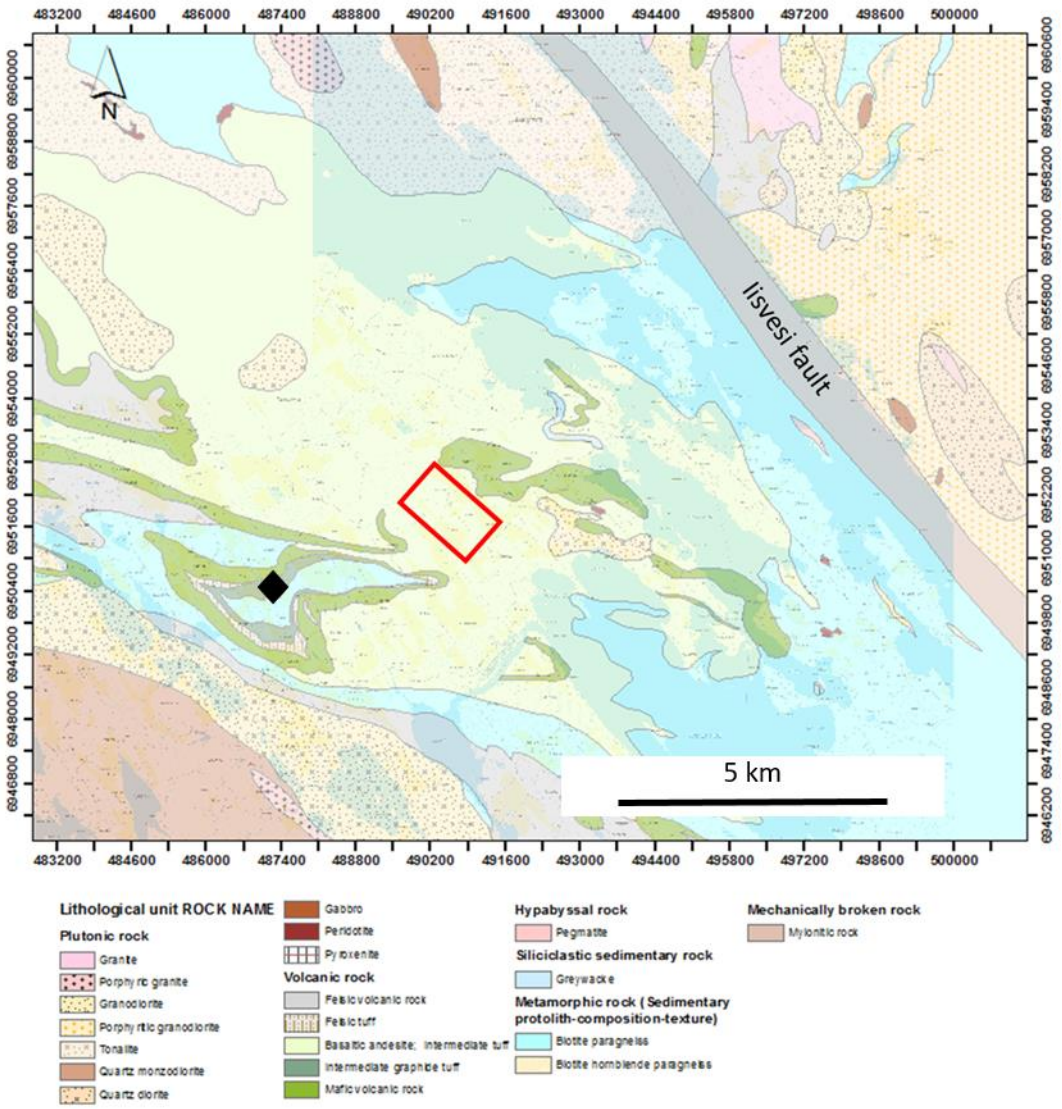

Figure 6. Geological map of the Rautalampi area. Study area Vaajasalmi marked with red rectangle and nearby Käpysuo graphite target with black diamond shape (Bedrock of Finland unscaled-DigiKP)

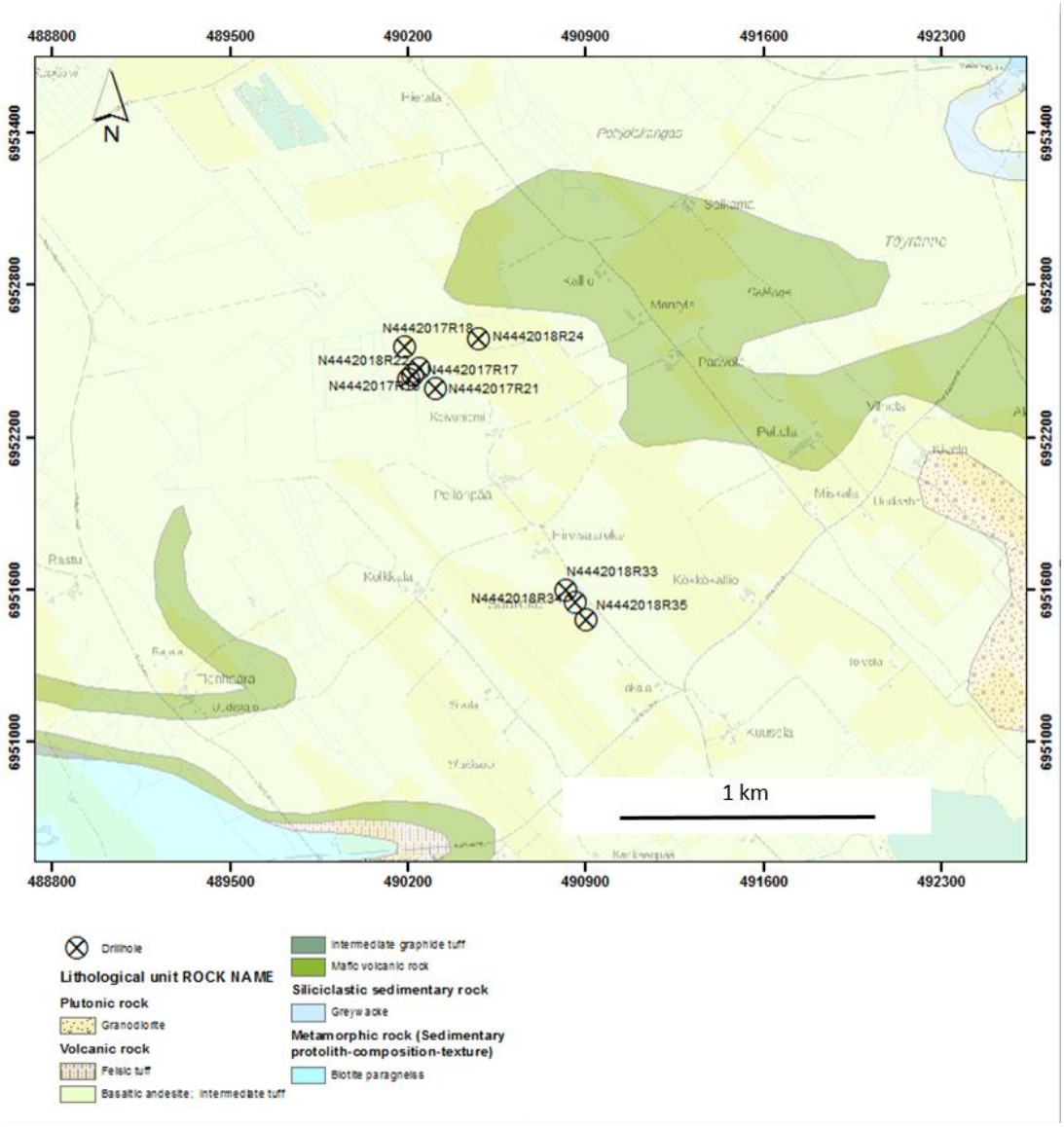

Figure 7. Geological map of the Vaajasalmi study area with locations of the drillholes (Bedrock of Finland unscaled-DigiKP). NW drill holes locate Koivuniemi target and SE drill holes are located at Saareke target.

Figure 8. Metamorphic facies map by Hölttä & Heilimo (2017). Study area is marked by red star (Metamorphic map 1:10 000 000, Bedrock of Finland- DigiKP).

4 Materials and methods

Study material in this study is concentrated on samples and analysis made from drill cores in the target area. Drill core loggings from the research area consist of 11 boreholes with 1178 m drill core logged by Janne Kuusela. A total of 16 thin sections were made for petrographic and mineralogical studies. GTK provided whole-rock sample data analyzed by Labtium Analytical Laboratories located in Kuopio. The carbon was analyzed with high temperature combustion technique (methods 816L and 811L). Broader set of unpublished analyses from same samples by GTK were used to complement and guide petrographic studies.

4.1 Petrographic analysis from thin sections

Thin sections from the target were prepared by GTK. The Vaajasalmi area consist of two different locations Koivuniemi and Saareke with minor differing in mineralogy. Samples from Koivuniemi consist of 12 thin sections and Saareke of four thin sections. The aim for the petrographic studies was to define microstructures, texture, mineralogy and to some extent paragenesis of the graphite and associated minerals. Thin sections were studied under the ore microscope with reflected and transmitted light at variating magnifications.

4.2 Scanning electron microscope and backscatter electron-images

Scanning electron microscope (SEM) was used to complement the petrographic studies and analyze the carbon concentration in graphite grains by using Energy Dispersive Spectrometer (EDS). This analysis was done with Thed Thermoscientific Apreo-S –scanning electron microscope. SEM-analysis was performed for four thin sections **(**N4442017R16 40.80, N4442017R18 32.30, N4442018R24 44.75 and N4442018R34 54.55), selected to represent different textures. The thin sections were cleaned with pressured air and attached to SEM compatible sled. Low vacuum drive (LoVac, 100Pa, H2O) was used in SEM analysis so the carbon coating was not needed. SEM-analysis was hosted by Ermei Mäkilä from The Physics department of University of Turku. Data was afterwards processed with Oxford Instruments AZtec (version 4.1) spectrum analysis software. Acquired spectrum was monitored and the elements were confirmed. The elements with less than 0,1Wt% were removed from the results to confirm reliability of the study. The Oxygen contents were omitted from analyse results.

Additional analysis for backscatter electron (BSE)-images of refractorial elements in graphite grains was performed with Phenom XL, Thermofisher, from the geology department of the

Åbo Akademi. SEM-EDS analyses were conducted by lab engineer Sören Frödjö and performed from 4 thin sections in low vacuum drive.

A scanning electron microscope works by focusing a high-energy electron beam on a sample. The atoms in the sample then send back some electrons based on the properties of the sample. These electrons can be detected by special electron detectors and an image can be constructed. The image is always black and white as the brightness of the image depends only on the intensity of the registered electrons. Depending on the instrument, a magnification of up to 500,000x can be reached. Such detail magnification is unachievable with optical microscopes. (Swapp 2017).

Backscattering electrons are the ones that are reflected from the sample by elastic scattering. BSE-images are notably lower in resolution, but the additional information is produced by recognition of different minerals due to the variable atomic number of the sample elements. EDS-analyzer is typically integrated into the SEM instrument. EDS-detector absorbs incoming x-ray energy. This energy yields conductive free electrons in the detector and produces an electrical charge bias. The absorption of x-rays produces different size electrical voltages which correspond to characteristic x-rays of variating elements. (Goodge 2017)

4.3 Raman spectroscopy

Raman analysis was performed on the four thin sections at Analytical Chemistry department of Åbo Akademi University with Rose-Marie Latonen as an operator. Analysis were run by Renishaw Ramascope with Leica DMLM microscope and CCD-camera equipped. The measurements were performed on the four previously selected thin sections (N4442017R16 40.80, N4442017R18 32.30, N4442018R24 44.75 and N4442018R34 54.55) to determine variation in quality of the graphite with differing metamorphic grade. Measurements were made for selected graphite grains with most probable perpendicular alignment to the C-axis (perpendicular to the graphene layers). In total, six grains were measured (two grains from samples N4442017R16 40.80 and N4442018R24 44.75 and singular grains from N4442017R18 32.30 and N4442018R34 54.55). The results are presented as spectrum with the Raman shift on the x-axis and the intensity on the y-axis. Obtained data was then processed with the Origin 2016 (64-bit) academic version. Peaks of the bands were determined with Lorentzian function of the Origin.

4.3.1 Theory of Raman spectroscopy

Raman spectroscopy is one of the principal methods for determining the quality of graphite. Method works by directing a laser beam of 514 nm wavelength onto a material. The individual atoms in the crystal lattice give rise to vibrations that can be read by a detector. These vibration bands are very sensitive to changes in the structure and bonds between atoms. Even small impurities can be seen as new, distorted or displaced vibrational bands (Wall, 2011).

Depending on the purity of the graphite material, it can give rise to several different peaks in the Raman spectrum that are characteristic of graphite (with 514 nm laser wavelength). Figure 9 shows an example of a spectrum with the names of the different peaks exposed. The spectrum can be divided into two categories, the first-order (1100-1800 cm-1) containing the spikes G, D, D' and the second order (2200-3400 cm-1) consisting of 2D (also called G'), D + D', D + D' and 2D'. When analyzing low metamorphism or low-quality graphite, peaks that are normally hidden below the G-peak in the spectrum can also be seen and they are then designated as D2, D3, D4 and the D-peak is designated as D1. It should be mentioned that the names of the various peaks have not been determined and other names may appear especially in older literature. (Antunes et al. 2006).

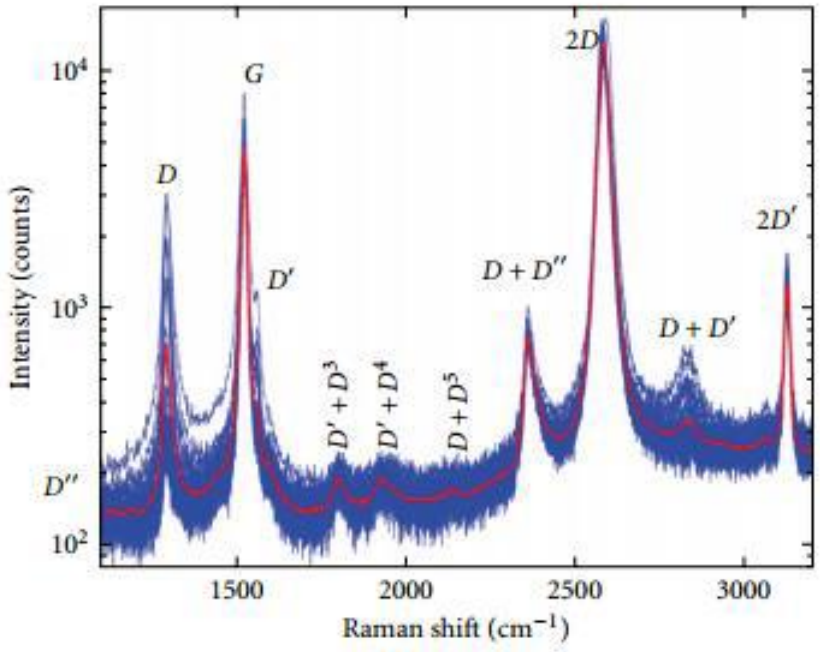

Figure 9. Example of Raman pattern and different bands. Blue area represent variability on the same sample whereas red line is the average band in that variability. The most important bands are the disorder band D and graphene structure quality band G (Olson 2015).

The D band (1360 cm−1) is known as the defect band or the disorder band. In graphite and high quality graphene, D band is commonly very weak. Major amount of defects (structural or impurities) in the material cause a rise and a widening in the band. D band is a resonant band with dispersive behavior. With different wavelength of a laser a different mode of a D band is enhanced (Wall, 2011). According to Aoya et al. (2010) the other disorder bands (D', D2, D3 and D4) are found next to the G-band.

The G band appears approximately at 1580 cm-1 in Raman spectrum. Carbon atoms forming graphene layers vibrate and the G band arises. The position of the G band is sensitive to the number of layers in the graphite grain. Quality of the graphite crystalline structure is typically led from the intensity ratio of D-and G-bands. Decreasing means shorter wavelengths and better crystalline structure quality (Antunes et al., 2006). In perfectly crystallized graphite the G band is the only peak emerging in the first region of the Raman spectrum (Beyssac et al., 2003)

The 2D band occurs in a range 2685-2725 cm-1 of Raman spectrum. The band is also called as G´ band since it is always observed in graphite samples with G band, but it is believed to represent the second order of the D peak and because of that some articles refer to it as 2D. With a single graphene layer, the 2D band is raising into a one symmetric peak. Multiple layers like in graphite the band is splitting into two subpeaks $2D_1$ and $2D_2$ (Ferrari, 2007).

Raman geothermometry is a method used to define the peak temperature of the metamorphism in which individual graphite grains were formed. Method is based on irreversible characteristics of the graphitization process. Temperature is the principle factor affecting the crystal structure of the graphite, whereas the pressure has only a minor effect (Beyssac et al., 2002). Heated organic matter expels hydrogen, nitrogen and oxygen from the system and carbon atoms form well-structured graphene sheets and in the end graphite. Several different equations have been presented to calculate metamorphic peak temperature. In this study, three different equations are used to ensure broad enough temperature range and to compare the results between the equations: 1. Beyssac et al. (2002), 2. Rahl et al. (2005) and 3. Aoya et al. (2010)

Beyssac et al. (2002)

$$R2 = \frac{D1}{G+D1+D2} \quad (1)$$

$$T\ (°C\ ) = -445 * (R2) + 641 \quad (2)$$

Rahl et al. (2005)

$$R1 = \frac{D1}{\mathrm{G}} \quad (3)$$

$$T(°C\ ) = 737.3 + 320{,}9 * (R1) - 1067 * (R2) - 80.638 * (R1)^2 \quad (4)$$

Aoya et al. (2010)

$$T(°C\ ) = 91.4(R2)2 - 556.3(R2) + 676.3 \quad (5)$$

5 Results

5.1 General petrographic description

Selected specimens for this study are listed in Table 1. The samples consist mainly of foliated metasediments. In the studied thin sections oriented biotite and graphite are the clear indicators of foliation. Typical major minerals in the studied specimens are quartz, plagioclase, K-feldspar and biotite, these are associated with graphite flakes. Graphite modal amounts varies between 1 % and 25 %, estimated by optical microscope. Other typical opaque minerals found in thin sections are pyrite and occasional pyrrhotite in relatively high concentrations, additionally chalcopyrite, sphalerite and rutile are found as trace amounts. In general, the grain size varies from fine to medium grain (0.1mm - <5mm) and graphite grain size correlate with surrounding minerals.

The graphite grains appear as angular, plate-like crystals and as swirly singular flakes or nodule-like aggregates in mica-rich schists and more coarse-grained gneissic variates. The graphite flakes typically appear along the boundaries of the other minerals and are commonly arranged parallel to other oriented minerals, especially biotite. The studied thin sections graphite flakes longest axis varied from 50 µm to 1000 µm. Quartz grains appear typically anhedral, granular and show features of recrystallization with mosaic texture, undulating distinction and elongated grains and clusters. The grains appear in all thin sections and coarse-grained quartz clusters with signs of recrystallization seem to be associated with the largest graphite flakes.

Biotite is found in all thin sections with widely variating modal amounts and grain sizes. Typically, the biotite grains are tabular, subhedral grains (2000 µm as longest axis) and the grains are often associated with graphite and sulphides.

Plagioclase is a common mineral in the specimens appearing as eu- and subhedral grains (100 µm – 1500 µm in diameter). K-feldspar appears as sub-angular grains (500 µm – 1500 µm in diameter) sporadically as microcline with cross-hatchet twinning. Both feldspars are typically moderately altered due to sericitization in hydrothermal processes. Seriticed feldspar clusters are often associated with the largest graphite flakes.

Sulphides appear in all studied thin section with pyrite as the most dominant. Other typical opaque minerals found in thin sections are occasional pyrrhotite in relatively high

concentrations, additionally chalcopyrite, sphalerite and rutile are found as trace amounts. The pyrite appears in groundmass as well as vein-like fillings. Individual grains are oriented parallel to a foliation of the rocks. Pyrite grains are often associated with graphite and biotite as they form parallel orientations. Occasionally, graphite flakes seem to be cutting pyrite grains and joint fillings indicating later crystallization. Pyrrhotite can be found as the dominant sulphide in one (N4442017R17 76.70) specimen. It is in the groundmass parallel to foliation and as joint filling, like pyrite. Chalcopyrite and sphalerite are common minerals, but their modal amounts are minor as they are found as small inclusions or associated with pyrite. In thin sections N4442017R16 68.40, N4442017R16 89.00 and N4442017R17 36.55 euhedral rutile with lamellar twinning is found in grains oriented parallel to foliation.

Table 1. Studied samples listed with graphite type (secondary type in brackets), mineralogy, estimated modal amounts of typical opaque minerals and carbon contents from whole rock-analysis measured with C analyzer after combustion pretreatment in 811L and HCL treatment in 816L.

Locality	Analyse number	Graphite type	Main gangue minerals	Accessory minerals	Graphite (modal amount)%	Py (modal amount %)	Po (modal amount)%	Carbon 811L (%)	C carb 816L (%)	C non carb 816L (%)
Koivuniemi	N4442017R16 40.70-41.70	3, 4, 5	Qtz, Bt, Plag		25	10		28.1	1.49	26.6
Koivuniemi	N4442017R16 68.40-69.40	1	Qtz, Bt, Plag, Sil	Rt	<1	4		0.3	<0.05	0.26
Koivuniemi	N4442017R16 89.00-91.00	4, 5	Qtz, Plag, Bt	Rt, Ms	10	15		8.45	<0.05	8.59
Koivuniemi	N4442017R17 36.55-38.55	3, 4	Qtz, Plag, Bt	Rt, Ms	20	10		15.5	0.19	15.3
Koivuniemi	N4442017R17 75.50-77.10	3, 4	Qtz, Bt, Plag, Sil	Ms	10		25	8.65	<0.05	8.92
Koivuniemi	N4442017R18 (Labtium-Analyse not found)	1	Qtz, Bt, Mc, Plag	Ms, Grt	3	2				
Koivuniemi	N4442017R18 94.80-96.10	5, (3)	Qtz, Plag, Bt		25	10		15.8	0.53	15.3
Koivuniemi	N4442017R21 19.15-21.15	1, (4)	Qtz, Plag, Bt, Mc	Grt, Zrn, Ap	1	4		0.82	<0.05	0.79
Koivuniemi	N4442017R21 43.65-45.65	1, (4)	Qtz, Plag, Bt, Mc	Zrn	1	9		0.55	<0.05	0.51
Koivuniemi	N4442017R21 64.00-65.60	5, (3)	Qtz, Bt, Plag		15	10		12.8	0.1	12.7
Koivuniemi	N4442018R22 71.00-72.60	5, (3)	Qtz, Plag, Bt, Ms		15	15		9.55	<0.05	9.54
Koivuniemi	N4442018R24 44.75-46.30	5, (3)	Plag, Qtz, Bt	Zrn	20	10		12.8	<0.05	12.9
Saareke	N4442018R33 38.20-40.20	2	Qtz, Plag, Bt, Hbl		7	12		4.47	0.07	4.4
Saareke	N4442018R34 52.80-54.70	2, (5)	Qtz, Plag, Bt, Aug, Chl		5	15		1.69	0.12	1.58
Saareke	N4442018R34 69.80-71.70	2	Qtz, Plag, Bt	Cb	6	22		4.47	0.49	3.98
Saareke	N4442018R35 37.00-38.70	2, (5)	Qtz, Plag, Bt, Hbl		5	15		2.54	0.21	2.33
	Abbrevations: Qtz-Quartz, Bt-Biotite, Plag-Plagioclase, Sil-Sillimanite, Mc-Microcline, Hbl-Hornblende, Aug-Augite, Chl-Chlorite, Ms-Muscovite, Grt-Garnet, Zrn-Zircon, Ap-Apatite, Cb-Carbonate, Rt-Rutile, Py-Pyrite, Po-Pyrrhotite	Graphite type: 1) small, narrow laths 2) singular swirly grains (Saareke) 3) large, plate like flakes associated with quartz and feldspars 4) joint filling flakes 5) swirly noodle-like aggregates ( )= secondary feature								

5.2 Detail petrographic description and division based on types of graphite

The graphite appears in various types through studied thin sections. In this study I divided those to five types that are latter described in more detail. These types include: 1) small to medium (<100-500 µm) and narrow lath-like grains in foliated rock with rather even distribution over the specimen, 2) small to medium-sized (<100-500 µm) swirly singular grains especially appearing in specimens from Saareke location, 3) large (500-1000 µm) long and plate-like flakes typically associated with quartz or feldspar clusters or major biotite stacks, 4) moderate-sized (~500 µm) grains forming joint fillings and 5) swirly graphite accumulations often accompanied with biotite. In the three latter types, the graphite is possibly partially or fully remobilized due to partial melting. These three types also often appear in the same specimens indicating to be formed in certain circumstances.

5.2.1 Detailed petrography of type 1 graphite samples

Small and narrow needle or lath-like graphite grains (Fig. 10) are found in four samples (N4442017R16 69.20, N4442017R18 32.30, N4442017R21 20.80 and N4442017R21 44.25), all from Koivuniemi site (Table 1). Microscopically samples are fine to medium grained (<1-2.5 mm), foliated, dominated by quartz, biotite, plagioclase and k-feldspar. Other minerals found from the samples are rutile, muscovite, sillimanite, garnet, zircons and apatite. Pyrite and graphite are the opaque minerals found from these samples with pyrite modal content of pyrite ranging from 2 to 9 % and graphite between 1-3 %. Graphite is strongly associated with biotite appearing next to or between biotite rich layers. Biotite and graphite grains are strongly oriented parallel to the foliation of the rock. Graphite flakes are ranging from 100 µm to 900 µm in size along the longest axis. Pyrite veins seem to cut general foliation in some samples but typically it is following the general foliation.

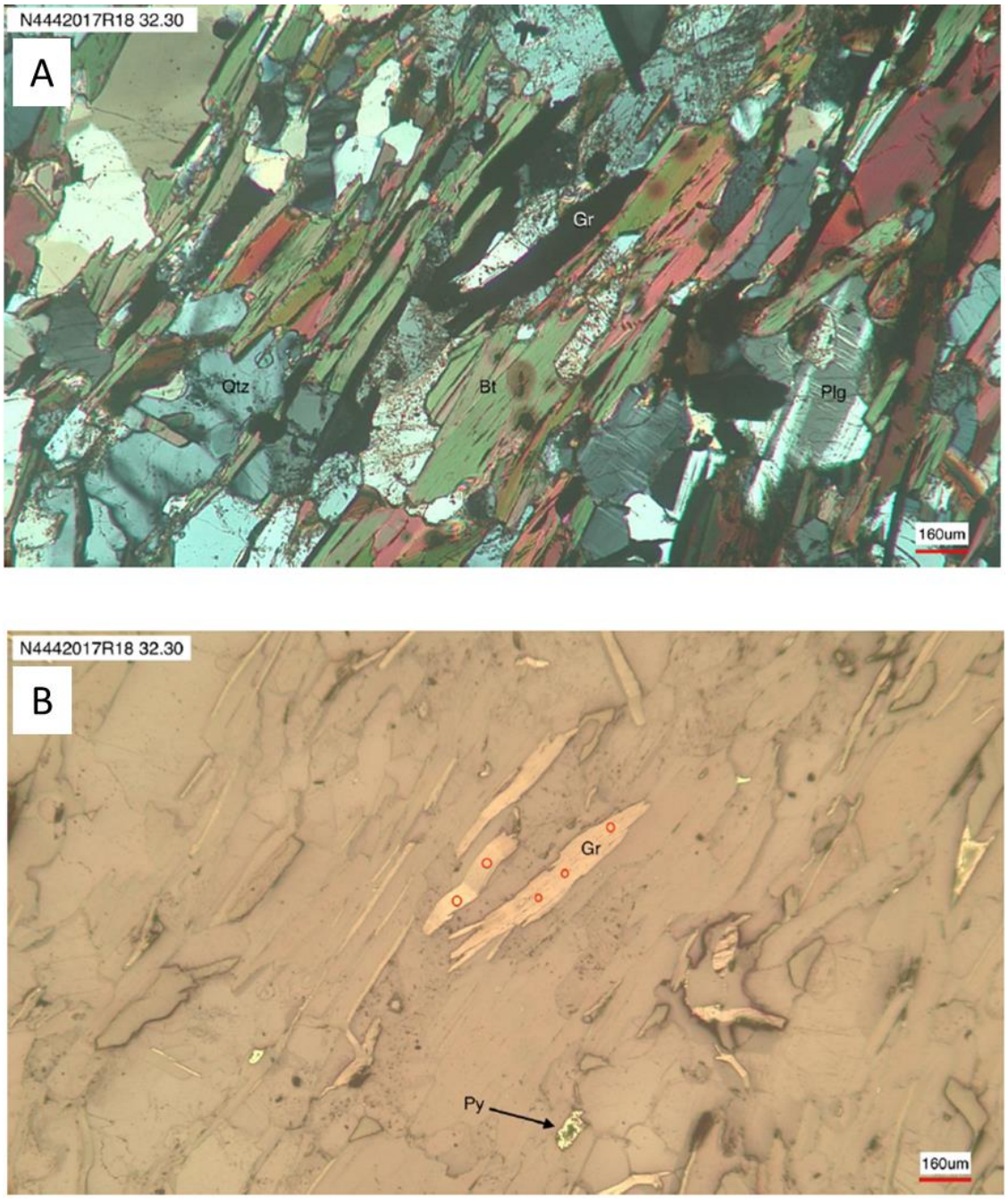

Figure 10. Photomicrograph of graphite type 1 in N4442017R18 32.30. Above (A) cross polarized image and below (B) reflected light image. Graphite grains (Gr) are oriented parallel to foliation and often associated with biotite (Bt)- rich layers. Pyrite (Py) appearing as small evenly distributed grains. Red circles indicate SEM-EDS –analysis spots.

5.2.2 Detailed petrography of type 2 graphite samples

All four samples from the Saareke target (N4442018R33 39.40, N4442018R34 54.55, N4442018R34 70.30 and N4442018R35 37.60) have similar features and graphite appearance represent a variation of types 2 and 5. The lithology is layered turbiditic metasediment and the layers vary from quartz dominating felsic layers to more mafic layers. Graphite grain size is

small to medium, appear typically as singular grains evenly distributed in the rock. Graphite flakes in the more mafic layers have swirly appearance and the singular flakes are not as parallel oriented to general foliation as in the Koivuniemi target rocks, but instead seem more disoriented (Fig. 11). Graphite often borders quartz, biotite or sericite altered feldspar. The modal amount of graphite in these four samples range from 5 to 7 % (Table 1). Other ore minerals found were pyrite, sphalerite and chalcopyrite. Pyrite is the most abundant with modal amounts from 12 percent to 22 percent. Pyrite appears typically as veins but also as euhedral grains. Sphalerite and chalcopyrite are found commonly from the edges of pyrite in veins and as inclusions in pyrite. Dominant gangue minerals are quartz, plagioclase, biotite, pyroxene, chlorite and hornblende. Quartz can be found as a ribbon-like elongated texture. In and in the vicinity of the pyrite veins, minor amount of carbonates (calcite/dolomite) was found. The rocks are moderately altered with sericitization and chloritization observed from samples. The alteration grade seems to affect graphite appearance as the intensively altered areas tend to contain more swirly- and disoriented graphite flakes.

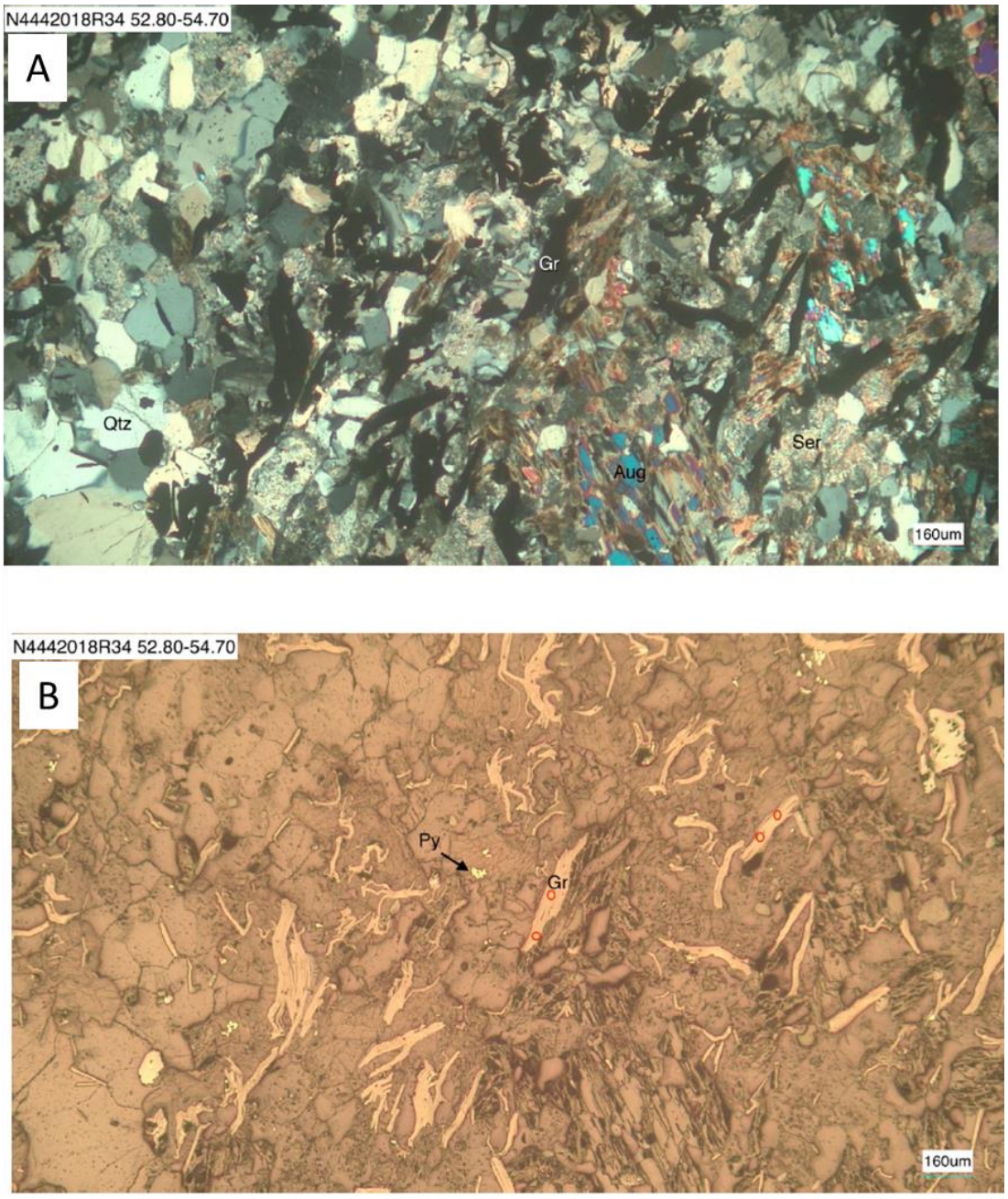

Figure 11. Photomicrograph of specimen N4442018R34 54.55 in cross polarized light-image (A) and reflected light- image (B). Type 2 graphite (Gr) appears as foliation- oriented, narrow, lath-like flakes and nodule-like aggregates. (Py)=pyrite, (Qtz)=Quartz.

5.2.3 Detailed petrography of type 3 graphite samples

Clear examples of type 3 graphite flakes are found from samples N4442017R16 40.80, N4442017R17 36.65, N4442017R17 76.70, N4442017R18 95.15, N4442017R21 64.75, N4442018R22 71.50 and N4442018R24 44.75. Macroscopically the samples are medium to coarse-grained, weakly foliated and contains a major amount of graphite and sulphides. Under the microscope, exact mineralogy consists of quartz, biotite and plagioclase as gangue

minerals (Fig. 12). Quartz grains are significantly larger than the grains of biotite and plagioclase. The modal amounts of graphite in these samples are among the highest of the studied thin sections (ranging from 10 to 25 %) and the size of the flakes is from 500 to 1000 µm in length. The coarse graphite flakes are typically associated with quartz grains that show features of grain boundary migration-type of recrystallization, due to undulating distinction and mosaic texture. Smaller graphite flakes (100-500 µm) are found as accumulations between coarser quartz aggregates and in joint fillings indicating remobilization via shear textures, formed between schistose layers. In joints, graphite is accompanied by fine-grained quartz, biotite and sericite.

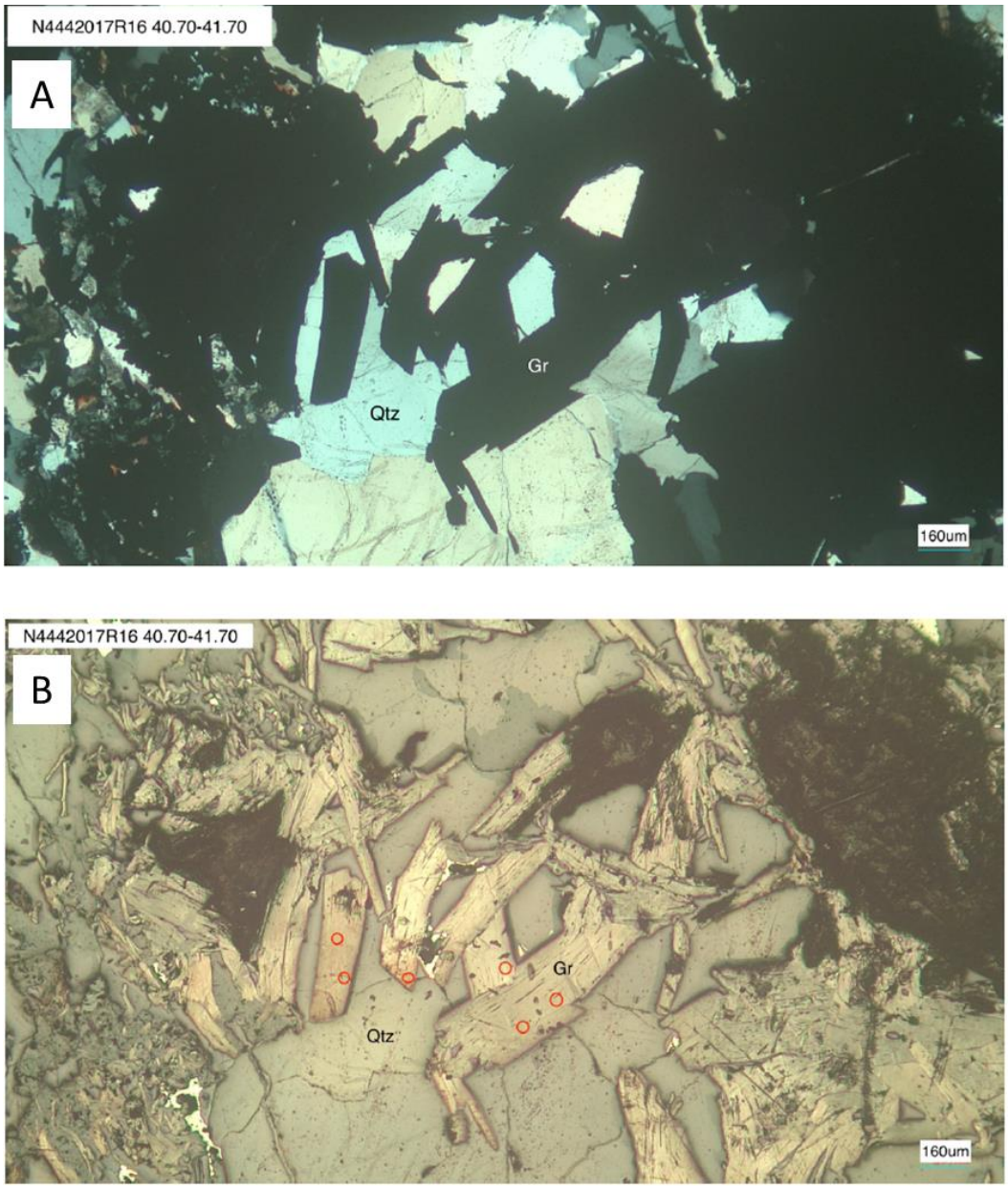

Figure 12. Type 3 Graphite in sample N4442017R16 40.80. A) cross polarized image and B) reflected light image. Large graphite flakes (Gr) are associated with quartz (Qtz) clusters. Red circles indicate SEM-EDS –analysis spots.

5.2.4 Detailed petrography of types 4 and 5 graphite samples

Type 5 graphite grains are common in medium to coarse-grained migmatite/ gneissic specimens showing strong deformational overprint. In total 8 samples represent this type of graphite appearance: N4442017R16 40.80, N4442017R16 90.90, N4442017R18 95.15, N4442017R21 64.75, N4442018R22 71.50, N4442018R24 44.75, N4442018R34 54.55 and N4442018R35 37.60. The grain size varies from 10 micrometer to millimeter scale in diameter. Coarse-grained parts of the rock show igneous looking texture with large feldspar and quartz grains (> 2 mm in diameter). Both feldspars are strongly altered to sericite and saussurite filled joint cuts sample N4442018R24 44.75 diagonally. Clear signs of partial melting are observed as graphite and biotite form swirly textures through thin section. Quartz grains are partly recrystallized showing undulating extinction and mosaic texture. The graphite occurs as large flakes (length 500 µm inside and on borders of sericite and quartz (Fig. 13), which is a similar feature to sample N4442017R16 40.80. Swirly graphite-biotite mass between coarse igneous-like areas look partially melted and remobilized.

Type 4 graphite grains are usually observed with swirly type 5, but type 4 graphite is not as clearly associated with biotite. Furthermore, grains of this type do not share the swirly outlook of type 5 and they seem to be controlled with faults and are accompanied with sulphides.

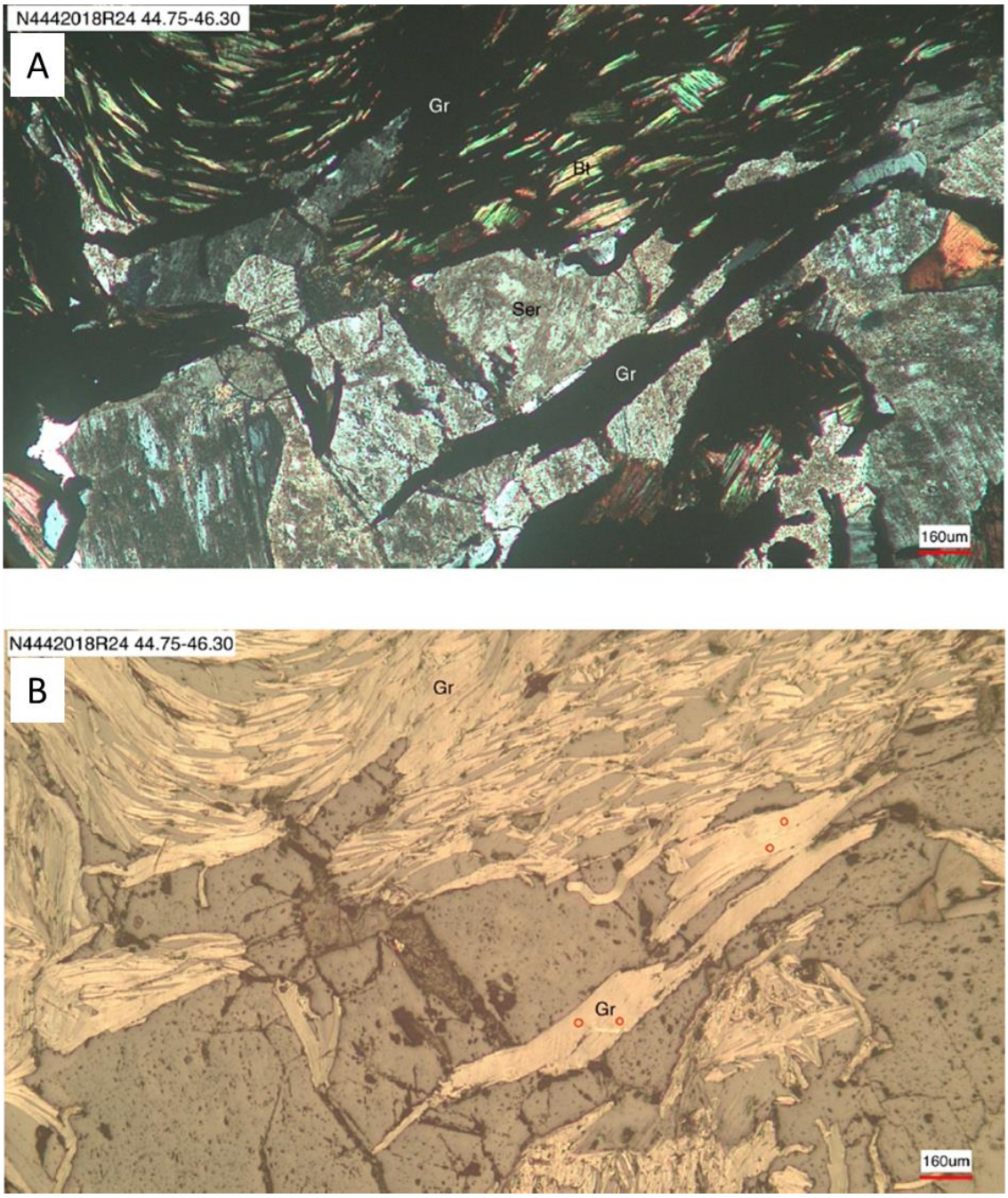

Figure 13. Photomicrograph illustrating features of graphite (Gr) appearing as large flakes and swirly aggregates due to partial melting associated with sericite (Ser) and biotite (Bt) in sample N4442018R24 44.75 representing the type 3 and 5 graphite types. Cross polarized light- image above (A) and reflected light- image below (B). SEM-EDS - analyze spots marked with red circles.

5.3 SEM-EDS results

Four thin sections were selected for the SEM-EDS analyses based on these differences representing partially the five appearance types of graphite flakes described in the

petrography sections. The aim was to measure the possible differences between graphite types (Appendix 1) as well as compare them to the whole rock carbon contents (Table 1).

SEM-EDS results type 3 graphite (Sample N4442017R16 40.80)

The analyzed spots were taken from graphite grains representing petrographical type 3 the largest long plate-like flakes (Fig. 12), associated with quartz and feldspar clusters. SEM-EDS analyses show high carbon content as it varies from 98.06 to 98.92 wt % (Appendix 2) and Si was the only other element above analyze limit in the flakes, content ranging from 1.08 to 1.36 wt %.

SEM-EDS results type 1 graphite (Sample N4442017R18 32.30)

Based on SEM-EDS analyses the carbon content range from 97.58 to 97.76 wt % in analyzed flakes of this sample (Fig. 10). The analyzed flakes are quite evenly distributed, small lath-like flakes representing petrographically type 1. Rest of the analysis (Appendix 2) show minor amounts of Na, Mg, Al, Si, K and Fe (max. total 2.42 wt %).

SEM-EDS results type 4 and 5 graphite (Sample N4442018R24 44.75)

The graphite flakes from the sample in Figure 13 contained 98.05-98.84 wt % of carbon (Appendix 2) and low amounts of impurities like Na, Al, Si, Fe, Mg. The analyzed spot represents a wide range of petrographical types 3-5. Several graphite minerals likely contained older inclusion of other rock-forming minerals grains.

SEM-EDS results type 2 graphite (Sample N4442018R34 54.55)

The carbon content of the SEM-EDS analyzed graphite grains shown in Figure 11 range from 97.09 to 97.7 wt % (Appendix 2). Low amounts of Fe, Al, Si, Mg and Ca can be found from analyses. This is likely due to remnants from surrounding pyroxene and sericite altered feldspars inside graphite flakes. The analyzed flakes represent type 2; small and narrow lath-

like disoriented swirly singular grains common in Saareke specimens and partly type 5; swirly nodule like aggregates.

5.4 Whole-rock analysis and drillhole profiles

Whole rock analysis were provided by GTK and analyzed by Eurofins Labtium Oy. The carbon content was analyzed using C analyzer with pretreatments of combustion and HCL in methods 811L and 816L respectively. Only drillholes selected to detailed petrographic study (N4442017R16, N4442017R18, N4442018R24 and N4442018R34) are processed in this chapter.

N4442017R16

The peak non-organic carbon content for this whole rock sample is 26.6 wt % (Table 1) which is the highest carbon value obtained in the study. In drillhole R16 the graphitic content increases in numerous layers (Fig. 14), suggesting multiple graphite rich layers which are intersected also in other nearby drillholes (R17 and R22).

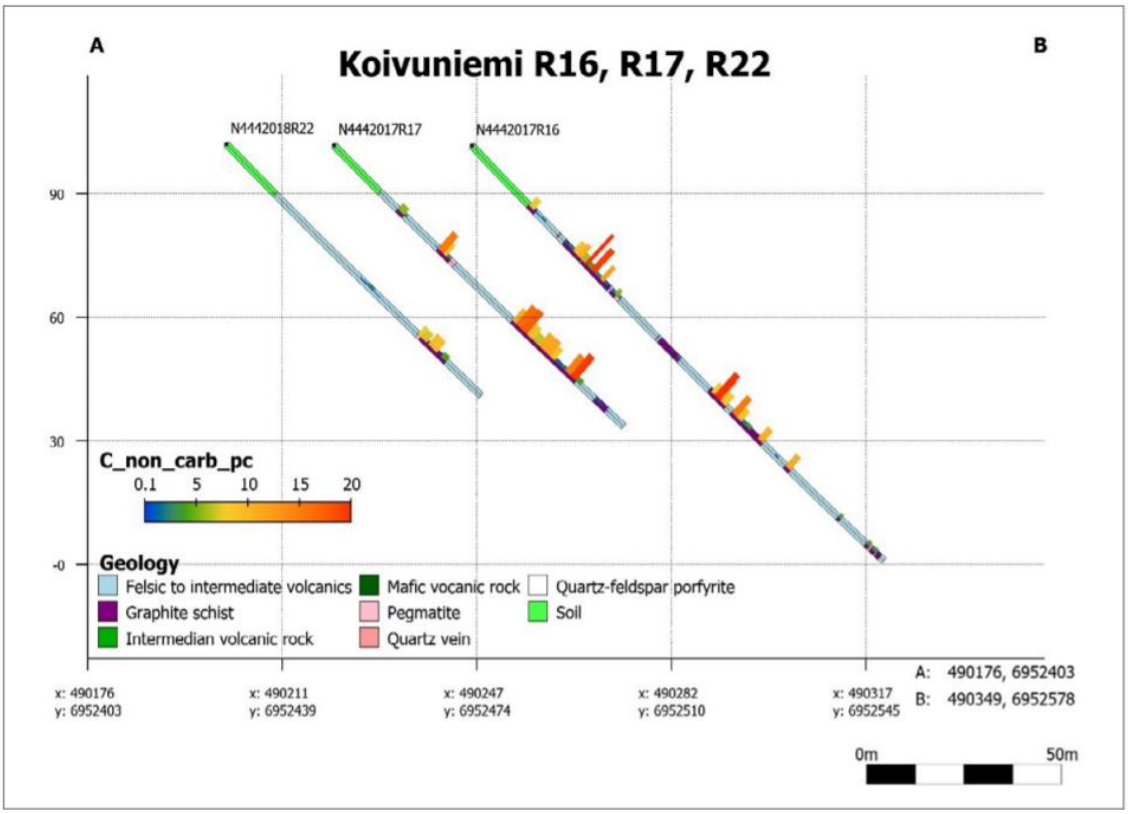

Figure 14. Drillhole profile and carbon content for three different drillholes R16, R17 and R22. Graphite rich layers are intersected in all holes with the highest carbon content reaching 26.6 % which represents the remobilized graphite types 3 and 5 described earlier in the study. (Kuusela et al., 2021)

N4442017R18

Unfortunately, the dataset does not contain whole rock analysis from the same depth as SEM result were achieved. The whole drillhole analysis is presented in Figure 15 showing the increase in content at the end of the drillhole.

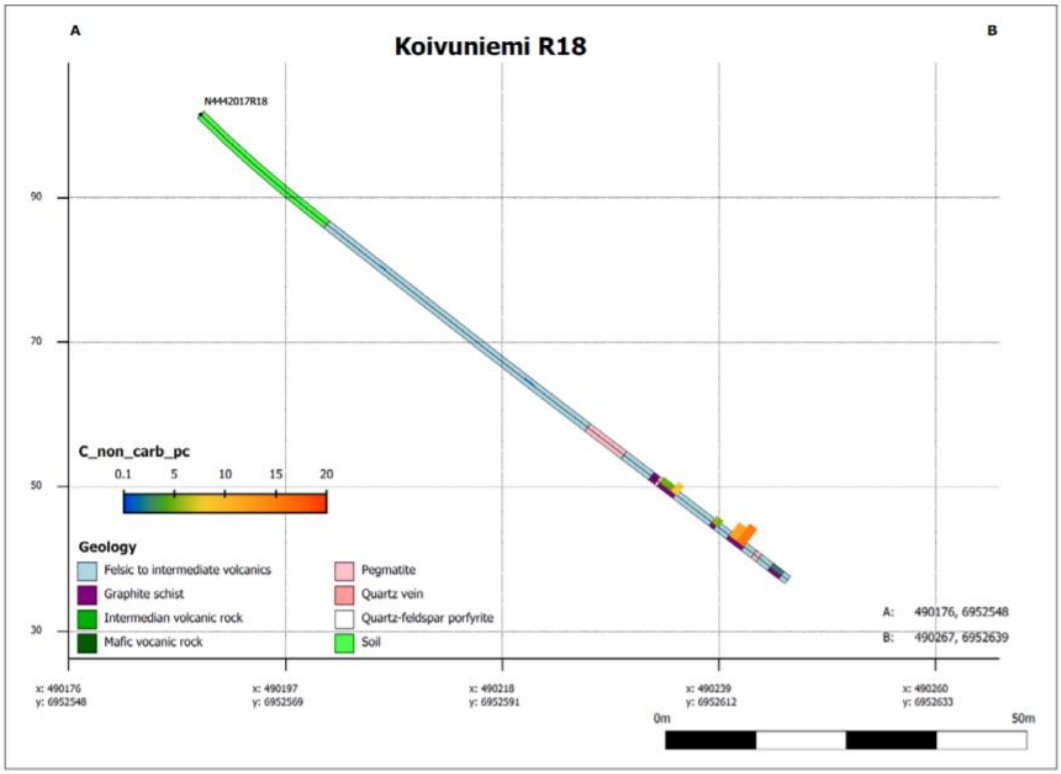

Figure 15. R18 drillhole profile with carbon contents. (Kuusela et al., 2021)

N4442018R24

Peak carbon content in this drillhole is 12.90 wt % (Table 1). The whole rock carbon content analysis for this core is presented in the Figure 16. This drillhole did not contain significantly graphite, only couple narrow graphite rich layers present.

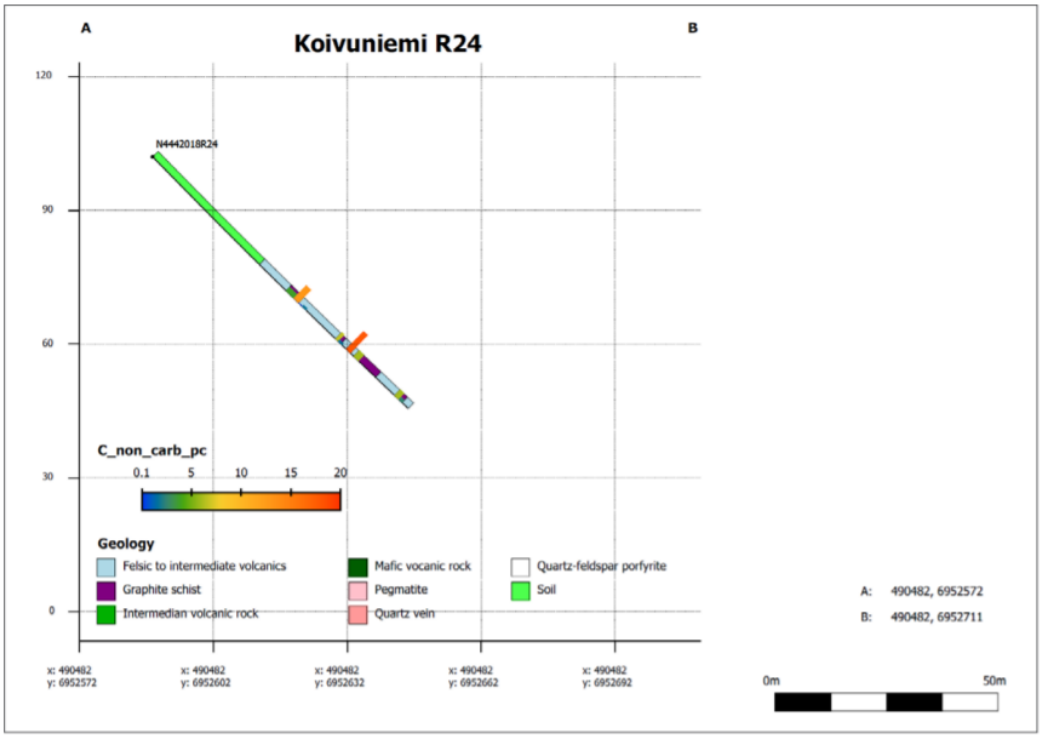

Figure 16. R24 drillhole profile which contain the type 5 graphite. Highest carbon content reached 17.9 % in this drillhole. (Kuusela et al., 2021)

N4442018R34

Non-organic carbon content in this drillhole stays below 5 wt % (Fig. 17) that complements also petrographical observations of modal amount. The carbon content raises in three localities throughout the drillhole, but the amounts are minor.

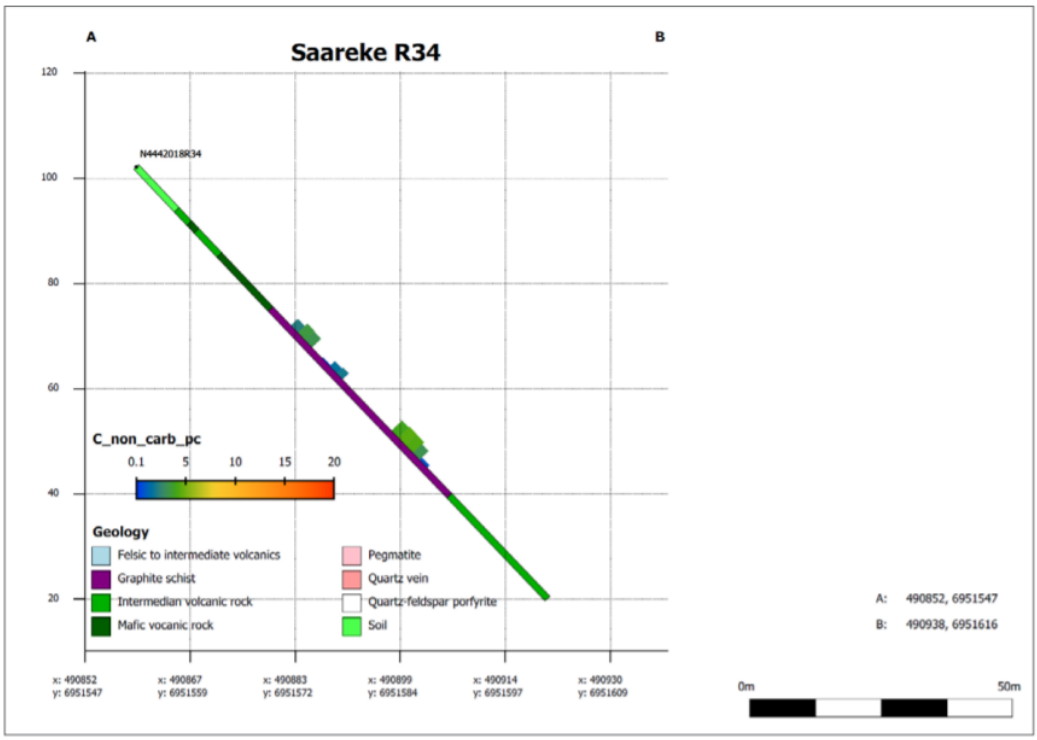

Figure 17. Drillhole profile with carbon content for the R34. Carbon content stays under 5% in this and in 3 other drillholes from Saareke target. (Kuusela et al., 2021)

5.5 Raman spectroscopy and geothermometer

Four thin sections N4442017R16 40.80, N4442017R18 32.30, N4442017R18 32.30 and N4442018R34 54.55 were analyzed in Raman spectroscopy. The first and third sample was analyzed from two different graphite grains and in two other samples only one grain from each was studied. Selected samples are the same ones used in SEM-analysis section to deepen the observations from different graphite flake types. All the analysed samples showed similar patterns in Raman spectroscopy (Fig. 18). Graphite bands are clear in all of the samples suggesting well-developed graphites. However, additional bands are observed in the spectra and these include the most common defect bands indicating disordered or impure graphite.

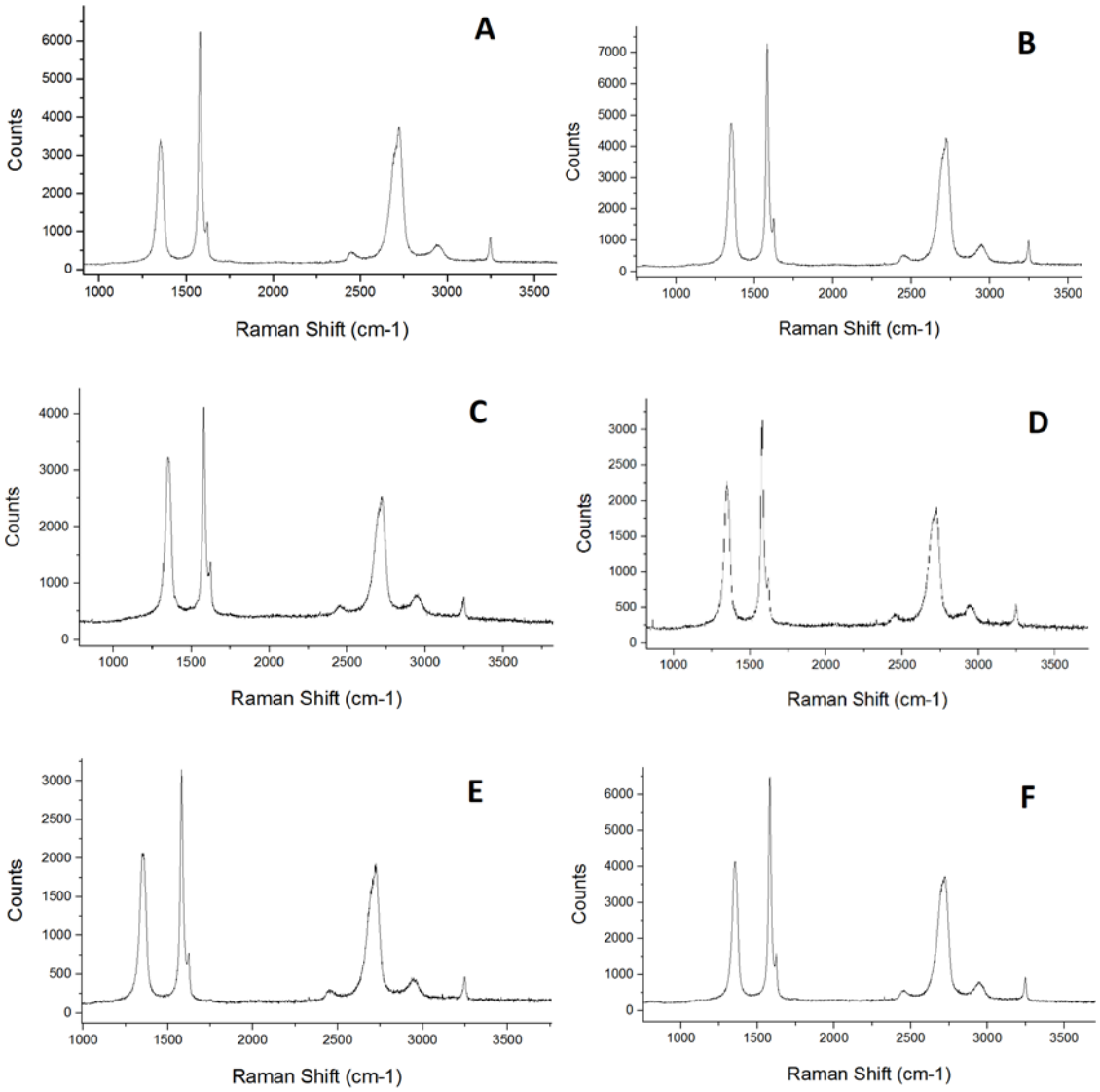

Figure 18. Raman patterns for the studied samples. A) N4442017R16 40.80A B) N4442017R16 40.80B, C) N4442017R18 32.30, D) N4442018R24 44.75A, E) N4442018R24 44.75B, F) N4442018R34 54.55. Similar patterns are observed throughout the analysis. Clear defect band D1 followed by sharp and intense G-band.

Calculations were proceeded according the three methods described earlier in this study. The areas and the intensities were obtained from the spectra to calculate the metamorphic temperature. All three methods gave similar but slightly different values (Table 2) ranging from the lowest 337.7 to highest 421.8 ºC. Methods by Beyssac et al. (2002) and Aoya et al. (2010) result to similar results with temperature differences between 1.5 and 2.5 ºC, whereas Rahl et al. (2005) method gives clearly lower temperature estimates resulting to differences between 50.7 and 61.6 ºC.

Raman spectra is divided into the first- and the second-order. In the first order-region clear D1 defect band is observed approximately at 1350 cm-1 showing structural or compositional

disorder in the graphite. The G-band is also clear and sharp exceeding the intensity of defect bands in every sample suggesting high quality of the graphite. This band is positioned approximately at 1580 cm-1 and it is showing symmetry in all samples indicating absence of the D3- band. The G-band is accompanied in every sample with clear, sharp but low intensity D2- band at ~1620 cm-1.

In the second- order the G*-band (fig. 9 D+D"-band) raises as a minor intensity peak at ca. 2440 cm-1 followed by asymmetric moderately high-intensity 2D-band (also called G') situated approximately at 2715-2725 cm-1. Peak forming at ca 2900 cm-1 is a combination of mode of the D and 2D bands. Last peak forming in the observed spectra is a sharp and narrow 2D'-band which is detected at 3245-3250 cm-1.

Table 2. Raman geothermometer results for three different methods from studied samples.

Sample	Beyssac ±50 ºC	Rahl ±50 ºC	Aoya ±30 ºC
N4442017R16 40.80 A	419.3	357.7	421.8
N4442017R16 40.80 B	398.2	337.8	400.0
N4442017R18 32.30	384.9	334.3	386.4
N4442018R24 44.75 A	399.4	347.4	401.2
N4442018R24 44.75 B	397.8	337.7	399.6
N4442018R34 54.55	406.2	352.4	408.3

6 Discussion

6.1 Comparison between targets

In this study, the aim was to determine mineralogy and origins of the Vaajasalmi area consist of two different local targets Koivuniemi and Saareke. Both targets represent metamorphosed sedimentary rocks, however samples from the Koivuniemi consist of paragneiss, whereas the Saareke contain more mafic volcanic interlayers. Second distinguished feature is found in appearance of graphite flakes, in Koivuniemi graphite appears in various types, whereas in Saareke mainly type 2 graphite and occasional type 5. Highest quality of the graphite grains was identified in type 3 with 98.92% carbon measured by EDS-analyzer.

Petrographic studies showed that the Koivuniemi target consist primarily of clearly foliated, fine to coarse grained paragneiss with variating migmatite composition indicating partial melting temperatures which in typical metapelites are in Svecofennian province above 650 ºC based pseudosection studies (Hölttä & Heilimo, 2017). Metamorphic index minerals sillimanite and garnet were observed occasionally in the studied samples.

Thin sections from the Saareke target represent probably turbiditic metasediments, where felsic mica schist layers and more volcanic mafic layers alternate. Volcanic layers contain hornblende, augite, chlorite and occasional carbonate suggesting clear seasonal volcanic sedimentary in the area.

Alteration grade varies from weak to strong, with no clear difference between Saareke and Koivuniemi targets. Sericitization, mainly in plagioclase is found from all the samples accompanied occasionally with saussuritization. Chloritization is found only from in rocks from Saareke. The alterations suggest retrograde metamorphism in the study area which is a common feature in the high grade graphites (Marchildon et al., 1993 according to Simandl et al., 2015).

Whole rock analysis show clear difference in carbon contents between the targets (Appendix 1). Non-organic carbon contents in Koivuniemi ranges from 0.26 to 26.6 wt % with 9.54 wt % median, whereas in Saareke from 1.58 to 4.4 wt % and 3.155 wt % median. Microscopically observed modal amounts of graphite are systematically higher than values from whole rock analysis.

According to SEM-EDS results the highest quality of graphite is in graphite grains associated with quartz and sericite altered feldspar clusters (Chapter 5.3 this study). This graphite flake type is presented earlier as type 3; large (500-1000 µm) long and plate-like flakes typically associated with quartz or feldspar clusters or major biotite stacks. Carbon content ranges from 98.02 wt% to 98.92 wt% in these graphite flakes with Si as only recognized impurity. Graphite flakes from Saareke contained 97.09-wt% 97.7 wt% of carbon. From the Saareke target the results are lowest values from the analysis indicating the impure quality of graphite. Impurities inside the Vaajasalmi graphite flakes typically contain the same elements as the minerals surrounding graphite, these include Si, Fe, Al and Mg. Graphite remobilization is a likely process based on the swirly texture and major accumulations of graphite in more intensively sheared rocks. It shows deformational localities that have been later filled with graphite and the small impurities might be derived from micro inclusions inside graphite flakes.

6.2 Raman analysis and geothermometer

In this study six graphite flakes were studied with Raman spectrometry to determine the quality of the flakes and estimate peak temperature for metamorphism from geothermometer (Table 2). Raman patterns do not really show variance in peaks and their relations but just in intensities of the peaks and some in asymmetry (Fig. 18). The bands presented in results section are located approximately in the same region in the Raman spectra in all samples.

Estimated temperature for the peak of metamorphism was calculated in three methods discussed in the material and methods stage. In the calculations the D1- band is a fundamental factor for the result and thus the highest value for temperature was 421.8 ºC obtained by Aoya et al. (2010) –method for the sample N4442017R16 40.80A (Fig. 12) which was considered as highest quality graphite flake in petrographic studies representing the type 3 graphite appearance. For the whole sample set the temperature estimate is approximately 400 ºC obtained with methods by Beyssac et al. (2002) and Aoya et al. (2010) which gave similar results. As expected the method by Rahl et al. (2005) led to lower estimations due the raised D1-band.

Disorder or defect bands are existing in every analysed Raman spectra (Fig. 18). The D1-defect band is apparent in all samples, indicating disorders in the structure of the graphite. Intense and wide D1 band is characteristic to poorly ordered graphites and its relative area tends to decrease as the graphitization process advance during metamorphism

(Beyssac et al. 2002), however the D3-band is absent in all samples suggesting peak of the metamorphism temperature above 450 ºC and moderately well-formed graphite (Beyssac et al. 2002). In the second order-region the 2D- band raises a clear and sharp peak with somewhat asymmetric left shoulder which is often associated with higher-grade samples and metamorphic temperatures exceeding 500 ºC (Beyssac et al., 2002).

The G-band which stands for the graphite peak is seen as sharp and narrow in every sample. It is also located in the region of ca. 1580 cm-1 on the Raman spectra which together with narrow and sharp peak indicate increased P-T- conditions (Beyssac et al. 2002). No variation between the targets was found in the Raman patterns and amount of defect bands suggest the moderate quality in the Vaajasalmi area graphite targets. However, according to Beyssac et al. (2002) the visible-light from the laser produce Raman scattering only in the uppermost parts of the sample, leading to sensitivity in the sample preparation. Especially the polishing stage of the thin section preparation affect the structural organization of the graphite, leading to raised defect bands. These observations are also noticed in the earlier studies on Svecofennian graphite targets e.g. Witick (2017) and Palosaari et al. (2020) where they observed significant differences in D1-band analysed from thin sections rather than from individual grains. Raised defect bands in every sample, possibly generated by structural discordance due to thin section preparation (Beyssac et al., 2002) leads to assumption of misleading metamorphic temperatures obtained from Raman geothermometer. Clearly elevated D1-band significantly lowers the temperature calculated by three geothermometer methods used in this study.

6.3 Regional P/T- estimation

The Vaajasalmi area graphite targets regional metamorphism conditions were estimated by mineralogical observations. Generalized P/T-pseudosections for average Svecofennian lithologies provided by Hölttä & Heilimo (2017) were used to constrain temperature and pressure conditions of the regional metamorphism. Differing lithologies between the targets were notified by using different pseudosection estimations for P-T conditions. Quartz recrystallization was observed in various thin sections and temperature estimation based on certain type recrystallization can be also used. In the metamorphic map of Finland (Hölttä & Heilimo, 2017) the study area is considered to represent granulite facies area (Fig. 8), but the observations from this study propose more upper amphibolite metamorphic conditions.

Since the Koivuniemi samples were identified as paragneisses rich in biotite and the Saareke rocks as volcanic layers containing metamorphosed sedimentary rocks, pseudosections for an

Al-rich pelitic rock and Archean amphibolite were respectively used from the metamorphic map of Finland (Hölttä & Heilimo, 2017).

Sillimanite and garnet minerals were found from the Koivuniemi biotite-rich paragneisses in thin section studies accompanied with moderate amount of melt. Therefore, I propose that the samples would fit into biotite-garnet-sillimanite+muscovite and <50% melt- field suggesting possibly moderate pressure field and the subfacies MP5.1 in the pseudosection made from average Svecofennian peltic rocks (Hölttä & Heilimo 2017; Fig. 19) with pressure ranging from 5 to 9.5 kbar and temperature above 650 ºC representing upper amphibolite facies. On an Archean amphibolite pseudosections (op. cit.) Saareke rocks fits into a low –pressure stability field LP5.3 (Fig. 20) of amphibole-clinopyroxene and plagioclase since hornblende, plagioclase and augite were found in all samples from the Saareke. Pressure in this field variates from <1 to 9.5 kbar and temperature from 500 to 750 ºC and rocks from Saareke probably represent the upper-end of this stability field.

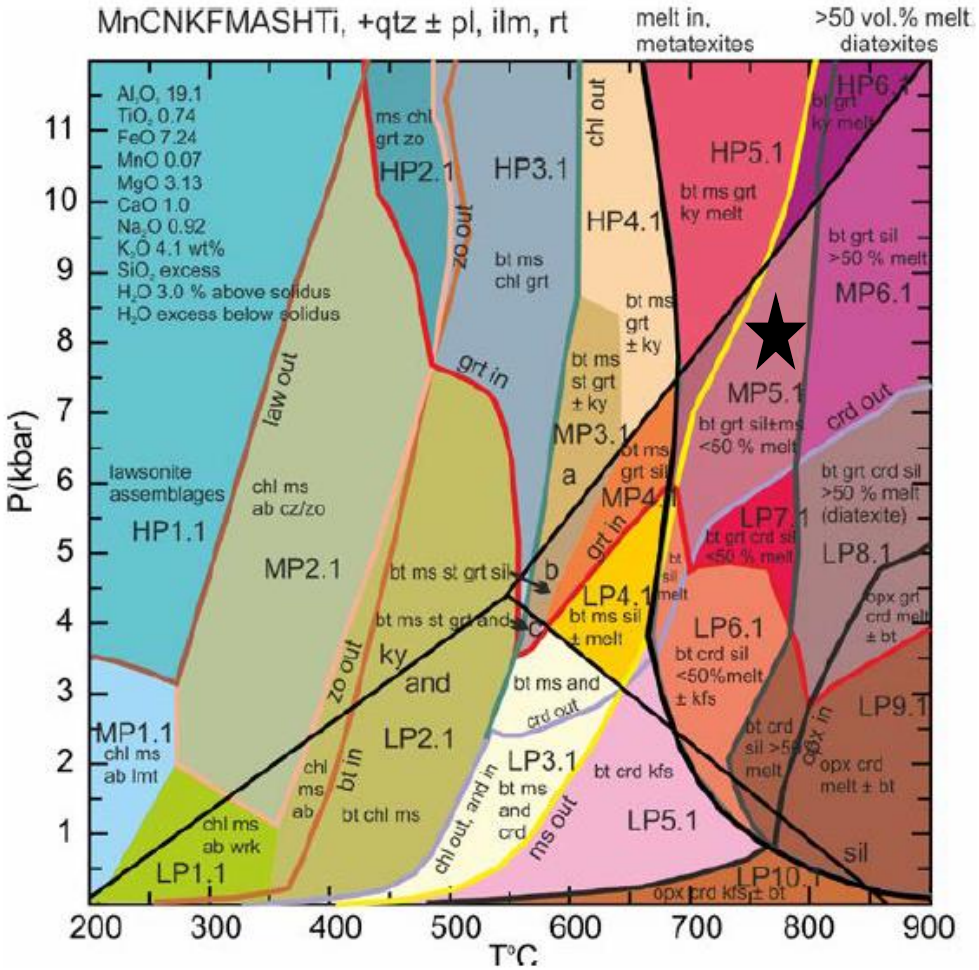

Figure 18. A generalized PT pseudosection for an Al-rich pelitic rock by Hölttä & Heilimo (2017). In the Koivuniemi target the MP5.1- metamorphic field (marked with black star) is proposed to represent the Koivuniemi target based mineralogy especially with abundant biotite, occasional garnet and sillimanite and moderate amount of melt in the thin sections.

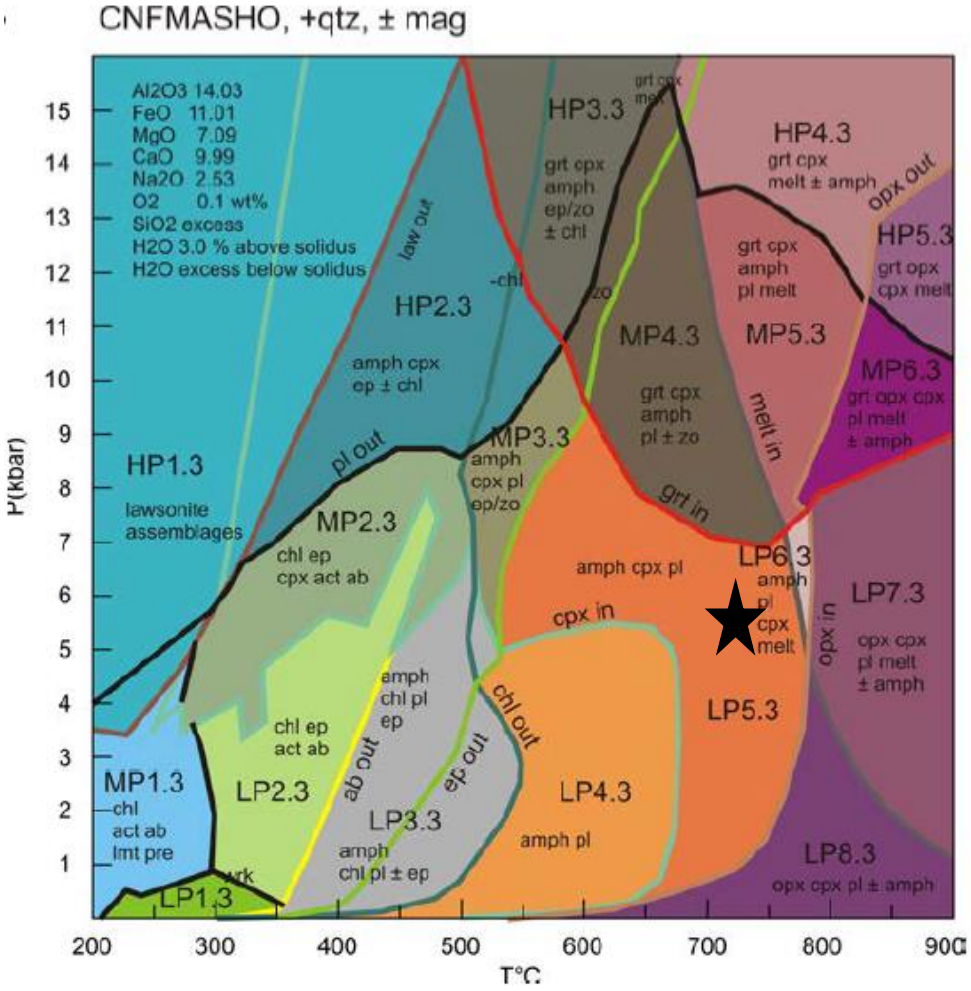

Figure 19. A generalized PT pseudosection for an average Archaean amphibolite by Hölttä & Heilimo (2017). Black star is marking the LP5.3- field which is considered to represent metamorphic conditions of the Saareke-target in the Vaajasalmi study area as clinopyroxenes, amphiboles and plagioclases were present in thin sections.

Largest and highest quality graphite grains in the Vaajasalmi seem to be associated with quartz appearing in recrystallized clusters (Fig. 12) showing features of chessboard-like undulating, indicating grain boundary migration- recrystallization (GBM). GBM-recrystallization forms irregular grain shapes and sizes. In the study area quartz grains are typically large or very large and large amplitude grain boundary sutures. Temperature estimate for GBM-recrystallization is above 550 ºC and extends to 700 ºC (Stipp et al., 2002). Chessboard extinction and large grains (Fig. 21) are typical for high temperature GBM 650 ºC. In a recent study only few kilometers west from Vaajasalmi study area by Al-Ani et al. (2021) they calculated peak P-T- conditions with pseudosection modelling with results ranging from 650 to 700 ºC. In Vaajasalmi area, graphite border quartz grains and penetrate

into clusters. This could be due the grain boundary migration forming large quartz grains with cracks for fluid carried remobilized graphite to intrude and mineralize.

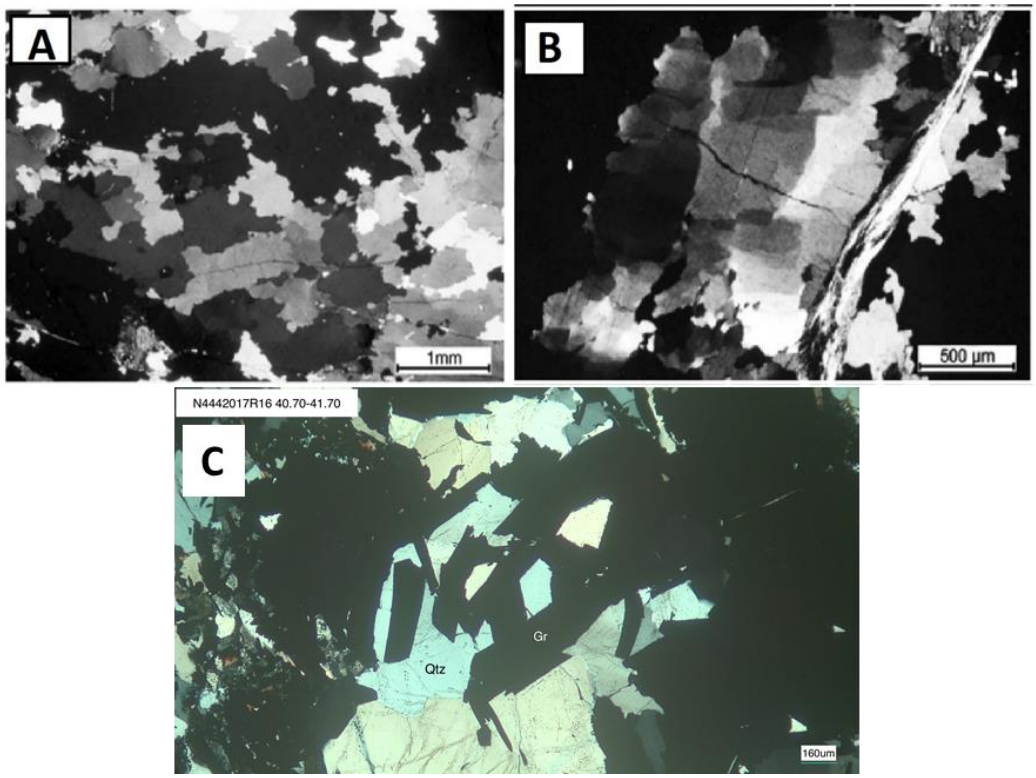

Figure 20. Grain boundary migration recrystallized quartz. A) Large grain sized irregular shaped, recrystallized quartz and B) chessboard extinction. These features typical for high temperature (~650°C) GBM Stipp et al. (2002), C) Sample N4442017R16 40.80 from study area with large quartz cluster (Qtz)with undulating extinction intruded by graphite (Gr).

6.4 Graphite genesis

According to Oohashi et al. (2011) graphite can enrich in two different ways in shear zones (Fig. 22): 1) In active type transporting via C, O and H- rich hydrothermal fluid graphite precipitate during cooling of the fluid in contact with the wall rock. The temperature required for C-O-H- fluid transportation is over 400 °C, which can be reached in sufficiently high metamorphism or at local increase in temperature due to shear zone friction. Precipitation of graphite typically takes place in fractures formed by shear zone and as the temperature drops to ca. 200 °C, precipitation of e.g. clay minerals fill in these dilational cracks. 2) The passive type consists of two different methods; pressure solution and diffusional mass transfer. In pressure solution minerals dissolve from higher pressure surfaces and transport to lower pressure areas like shear zones. Diffusional mass transfer is movement of mass due to the motion of atoms and molecules. Impurities in the crystal lattice migrate out in progressive

deformation causing raising temperature and pressure. Passive type is a slow enrichment type, considered to take millions of years per meter of transportation. Process of passive type enrichment is presented in Figure 22a. Host rock is a graphite-bearing biotite-paragneiss where fluids start to flow in cracks produced by shearing. In progressive shearing, the pressure drops causing water-soluble substances like calcium and silica to migrate away and leading to enrichment of insolubles like graphite, mica and opaque minerals.

In general graphite can be found typically with biotite and it is enriched in biotite-rich layers in gneisses/schists in the Vaajasalmi area. Graphite flakes are often bordering other mineral grains seeming to occur freely. The largest graphite flakes often appear with quartz and moderately altered plagioclases and K-feldspars (Figs. 12,13) and are typically associated with remobilized-looking, swirly, medium-sized graphite flakes appearing with biotite (Fig. 13) representing graphite appearance types 3, 4 and 5 in this study. As these graphite-biotite enrichments seem to be filling fractures with other opaque minerals, often pyrite with minor chalcopyrite occurring on edges of pyrite grain, it is suggesting possible hydrothermal fluid flows through the system.

Examples of the graphite enrichment in paragneiss via deformation studied by Oohashi et al. (2011) are presented in Figure 23. Thin sections from Vaajasalmi study look very similar with type 1 small, evenly distributed narrow flakes sitting in paragneiss to remobilized looking graphite-biotite accumulations of type 3 and 5 graphite flakes situated in fractures (Fig. 24). The Vaajasalmi area is in the vicinity of Raahe-Laatokka suture zone, which has affected the local bedrock with various fractures and faults (Koistinen & Vihreäpuu 1982). These structural features enable major fluid flow channel forming and therefore potential enrichment zones for graphite.

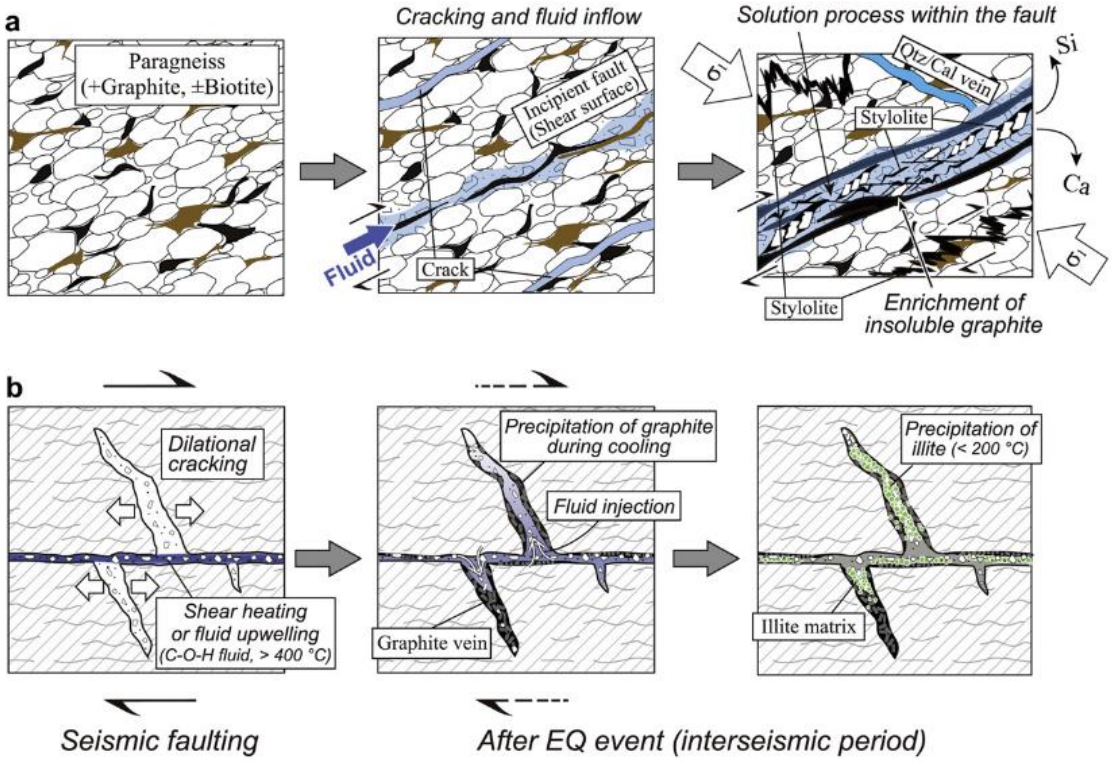

Figure 21. a) A passive way to enrich graphite in shear zones. When shear occurs in a paragneiss is transported water-soluble minerals are removed and there is an enrichment of insoluble minerals such as graphite. b) An active way to enrich graphite in shear zones. Hydrothermal solutions precipitate graphite during cooling in contact with the side rock (Oohashi et al., 2011).

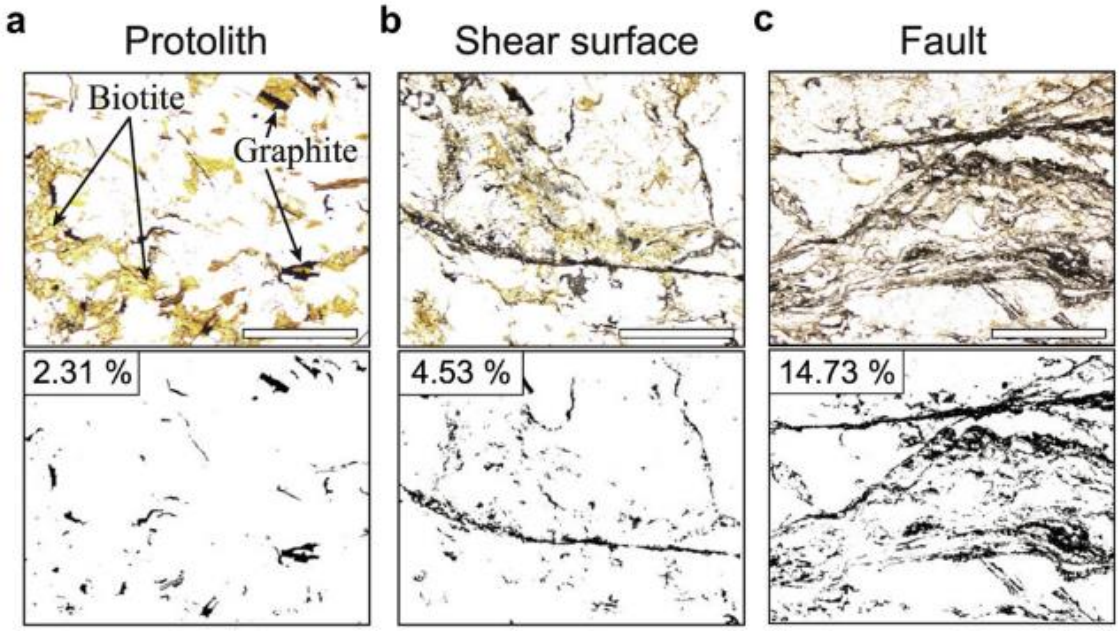

Figure 22. Examples how the amount of graphite increase as the deformation progress in paragneiss. a) Protolith stage with no or early deformation b) shearing and graphite enrichment along the fault surface c) a well-developed shear or rejection with clear enrichment of graphite (Oohashi et al., 2011).

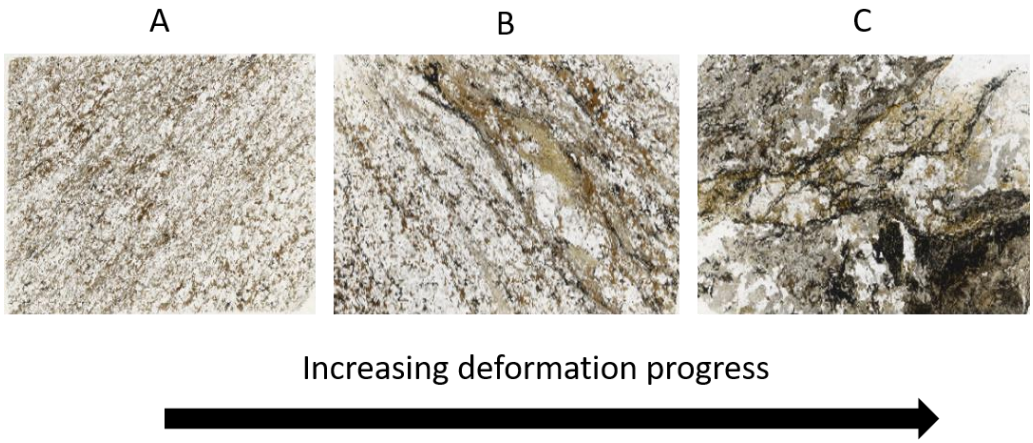

Figure 23. Samples N4442017R21 44.25 (A): N4442017R18 32.30 (B): N4442018R24 44.75 (C) from the Vaajasalmi target in a photo serie of showing an increased shear and enrichment of graphite. The image series illustrate clear similarity to Figure 23 (Oohashi et al. 2011) in the shear development and graphite enrichment.

In this study, impurities inside the graphite flakes typically contain the same elements as the minerals surrounding graphite, these include Si, Fe, Al and Mg (Appendix 1). The graphite remobilization is clearly process in Vaajasalmi based on the texture that shows deformational localities, dilational cracking which are filled with graphite (Fig. 21).

In SEM-studies inclusions inside graphite grains seem to situate parallel to flakes longest axis, (Fig. 25), possibly between weak van der Waals bonded of graphene layers (Fig. 2). However, due to limitations of the resolution in the SEM back-scattered electron images made it impossible to observe very small inclusions inside graphite. Recent study from the Vaajasalmi area was conducted by Kuusela et al. (2021) showed residues of 0.3-0.4 % of SiO_2 after purification tests which could be due the quartz inclusions inside graphite grains (Fig. 25).

Figure 25. A backscattered electron microscope image of typical elongated inclusion inside a graphite grain. Spot analysis from the + mark showed elevated values of S, Fe, Si, and Al.

7 Conclusion

The Vaajasalmi study area consists of two graphite targets; locally graphite-rich biotite-paragneiss at Koivuniemi target and moderately graphite-bearing metamorphosed sedimentary rock with volcanic interlayers at Saareke target. Graphite appears in types: in Koivuniemi 1) small and narrow singular lath-like grains, 3) large, plate-like flakes associated with quartz and sericite altered feldspars, 4) remobilized graphite- appearing with pyrite in joint fillings and 5) swirly, noodle/like medium to coarse grained remobilized flakes associated with biotite. The Saareke target graphite appears as swirly singular graphite flakes of type similar to the type 2.

Petrographic studies and mineralogical comparison to the metamorphic pseudosection from Finnish Svecofennian rocks suggest upper amphibolite facies metamorphic conditions in the Vaajasalmi study area. The temperature might have been in range of 650-750 °C and pressures between 5 and 9.5 kbar. The estimation is supported by abundant amount of grain boundary migrated recrystallized quartz observed from thin sections.

Based on interpret metamorphic conditions and petrographical study graphite in the Vaajasalmi area is remobilized by C-O-H-fluids in deformational processes and enriched in the dilational cracks in the host rock. The enrichment is clearly visible in the thin-sections showing more intensive shearing. According to scanning electron microscope studies the remobilization of graphite seems to lead to better quality graphite flakes and at the same time grain size and modal amount of carbon increase.

Remobilized graphite types 3 and 5 show the greatest potential for economical interest. The largest flakes were found in clusters of recrystallized quartz and sericited feldspars, suggesting graphite enrichment in structurally weak areas. The impurities inside the graphite flakes are possibly due to inclusions inside the crystal structure of remobilized graphite.

Raman spectrometry analysis gave contradictory results, due to poor graphite structure related to the making of the thin section.

Acknowledgements

I would like to thank you my supervisors, Esa Heilimo (University of Turku) and Janne Kuusela (Geological survey of Finland) well as operators of Raman, Rose-Marie Latonen (Åbo Akademi) and Scanning Electron Microscopes Ermei Mäkilä (University of Turku) and Sören Fröjdö (Åbo Akademi). Thank you also to Olav Eklund (Åbo Akademi) for providing great insights on graphite. Warm thank you and big hand to everyone at Geohouse.

References

Ahtola, T. & Kuusela, J. 2015: Esiselvitys Suomen grafiittipotentiaalista. Geological Survey of Finland. Open file report 88/2015. 14 p. (In Finnish)

Al-Ani, T., Ahtola, T., Cutts, K. & Torppa, A. 2021: Metamorphic evolution of graphite in the Paleoproterozoic Savo Schist Belt, Central Finland: Constraints from geothermetric modeling. Ore Geology Reviews

Aoya, M., Kouketsu, Y., Endo, S., Shimizu, H., Mizukami, T., Nakamura, D. & Wallis S. 2010: Extending the applicability of the Raman carbonaceous-material geothermometer using data from contact metamorphic rocks. Journal of metamorphic geology 28, 895-914.

Antunes, E. F., Lobo, A. O., Corat, E. J., Trava-Airoidi, V. J., Martin, A.A. & Veríssimo, C. 2006: Comparative study of first- and second-order Raman spectra of MWCNT at visible and infrared laser excitation. Carbon 44, 2202-2211.

Beyssac, O., Goffé, B., Chopin, C. & Rouzaud, J.N. 2002: Raman spectra of carbonaceous material in metasediments: a new geothermometer. Journal of Metamorphic Geology20, 859-871.

Beyssac, O., Goffe, B., Petitet, J-P., Froigneux, E., Moreau, M. & Rouzaud, J-N. 2002: On the characterization of disordered and heterogeneous carbonaceous materials by Raman spectroscopy. Spectrochimica Acta Part A 59, 2267-2276.

Eriksson, M. 2018: Determening the metamorphic degree around graphite occurences in the Heinävesi area. Åbo AkademiUniversity ,81 p. (Unpublished Master's thesis)

European Commission 2020: Study on the EU's list of Critical Raw Materials (2020). Critical Raw Materials Factsheets 341-368.

Ferrari, A. C. 2007: Raman spectroscopy of graphene and graphite: Disorder, electron–phonon coupling, doping and nonadiabatic effects. Solid State Communications 143, 47-57.

Goodge, J. 2017: Energy-Dispersive X-Ray Spectroscopy (EDS). University of Minnesota-Duluth. [https://serc.carleton.edu/research_education/geochemsheets/eds.html]. Accessed 13.10.2021.

Hölttä, P.S. & Heilimo, E. 2017: Metamorphic Map of Finland. Geological survey of Finland. Special paper 60, 77-128 p.

Koistinen, T. & Vihreäpuu, U. 1982: Suonenjoki ja Rautalampi lentoalue I-II 1975-1982. Outokumpu Oy 432. 253 p. (In Finnish)

Kuusela, J., Salvador, D., Nurkkala, J., Heilimo, E., Nousiainen, M., Ahtola, T. & Al-Ani, T. 2021: The Vaajasalmi flake graphite, Rautalampi, Central Finland. Geological Survey of Finland, Open File Research Report 60/2021, 34 p.

Kähkönen, Y. 1998: Chapter 7 Svekofenniset liuskealueet – merestä peruskallioksi. In: Lehtinen, M., Rämö, O.T. Nurmi, P. (Eds.) Suomen kallioperä: 3000 vuosimiljoonaa. Suomen Geologinen Seura ry., 199-227. (In Finnish)

Lahtinen, R. 1994: Crustal evolution of the Svecofennian and Karelian domains during 2.1–1.79 Ga, with special emphasis on the geochemistry and origin of 1.93- 1.91 Ga gneissic tonalites and associated supracrustal rocks in the Rautalampi area, central Finland. *Geo*logical Survey of Finland Bulletin 378, 128 p.

Laitakari, A. 1925: Die Graphitvorkommen in Finnland und ihre Entstehung. Geologinen Komissioni. Geoteknillisiä julkaisuja. N:o 40. 106 p. (In German)

Lehtinen, M., Nurmi, P. & Rämö, O.T. 1998: Suomen kallioperä: 3000 vuosimiljoonaa. Suomen Geologinen Seura ry, 375 p. (In Finnish)

Marchildon, N., Simandl, G.J. & Hancock, K.D. 1993: The AA graphite deposit, Bella Coola area, British Columbia: exploration implications for the coast plutonic complex. In: Geological Fieldwork 1992, British Columbia Ministry of Energy and Mines, British Columbia Geological Survey Paper 1993-1, 389-397.

Nironen, M. 2017: Guide to the Geological Map of Finland – Bedrock 1:1 000 000. Geological survey of Finland, Special paper 60, 41-76.

Nurmela, P. 1989: Katsaus Suomen grafiittiesiintymiin. Geologian tutkimuskeskus Arkistoraportti M81/1989/1. 21 p. (In Finnish)

Nygård, H. 2017: Kvalitetsbestämning av flakgrafit i Haapamäki, Leppävirta, Norra Savolax. Åbo Akademi University 69 p. (Unpublished Master's thesis in Swedish)

Oganov, A., Hemley, R., Hazen, R. & Jones, A. 2013: Structure, Bonding, and Mineralogy of Carbon at Extreme Conditions. Reviews in Mineralogy and Geochemistry 75(1), 47-77.

Olson, D. 2015: Graphite - Advance release. 2013 Minerals Yearbook. U.S. Geological Survey, 32.1-32.12.

Oohashi, K., Hirose, T., Kobayashi, K. & Shimamoto, T. 2011: The occurrence of graphite-bearing fault rocks in the Atotsugawa fault system, Japan: Origins and implications for fault creep. Journal of Structural Geology 38, 39-50 p.

Palosaari, J., Latonen, R-M., Smått, J-H., Raunio, S., & Eklund, O. 2020. The flake graphite prospect of Piippumäki—an example of a high-quality graphite occurrence in a retrograde metamorphic terrain in Finland. Mineralium Deposita. 55. 1647-1660.

Puronaho, L. 2018. Structural interpretation of graphite-bearing black schist in Aitolampi area, Eastern Finland. Åbo Akademi University. 64 p. (Unpublished Master thesis)

Puustinen, K. 2003. Suomen kaivosteollisuus ja mineraalisten raaka-aineiden tuotanto vuosina 1530- 2001, historiallinen katsaus erityisesti tuotantolukujen valossa. Geologian tutkimuskeskus. Arkistoraportti, M10.1/2003/3. 578 p. (In Finnish)

Rahl, J., Anderson, K. M., Brandon, M. T. & Fassoulas, C. 2005: Raman spectroscopic carbonaceous material thermometry of low-grade metamorphic rocks: Calibration and application to tectonic exhumation in Crete, Greece. Earth and Planetary Science Letters 240, 339-354.

Sarapää, O. & Kukkonen, I. 1984. Grafiittitutkimukset Kiihtelysvaaran Hyypiässä vuosina 1981 - 1983. Geologian tutkimuskeskus. Arkistoraportti M81/4241/-84/2. 30p.

Sarapää, O. & Kukkonen, I. 1984. Grafiittitutkimukset Juuassa vuosina 1982 - 1983. Geologian tutkimuskeskus. Arkistoraportti M81/4311/-84/1.

Simandl, G.J., Paradis, S., Akam, C. 2015. Graphite deposit types, their origin, and economic significance. British Columbia Ministry of Energy and Mines & British Columbia Geological Survey. 163-171.

Stipp, M., Stunitz, H., Heilbronner, R. & Schmid, S. 2002. The eastern Tonale fault zone: a ´natural laboratory´ for crystal plastic deformation of quartz over a temperature range from 250 to 700 ºC. Journal of Structural Geology. 24. 1861-1884.

Swapp, S. 2017: Scanning Electron Microscopy (SEM). University of Wyoming. [https://serc.carleton.edu/research_education/geochemsheets/techniques/SEM.html]. Accessed 13.10.2021.

Wall, M., 2011. The Raman Spectroscopy of Graphene and the Determination of Layer Thickness. Thermo Fisher Scientific, WI, USA. 5 p.

Witick, I. 2017: The Occurrence and Characterization of Graphitic Carbon in Southern Tuusniemi, South-Eastern Finland. Åbo Akademi University,. 49 p. (Unpublished Master's thesis)

Appendices

Appendix 1. Detailed list of petrographical observations and carbon contents of whole rock-analysis.

Locality	Analyse number	Sample number	Thin section number	Graphite appearance	Graphite (%)	Quartz (%)	Plagioclase (%)	K-feldspar (%)	Biotite (%)	Muscovite (%)	Other mineral (%)	Pyrite (%)	Pyrrhotite (%)	Accessory/ trace minerals	Alteration 1	Alteration intensity	Alteration 2	eration 2 intens	Alteration 3	eration 3 inten	811L (wt %)	816L (wt. %)	816L (wt %)
Koivuniemi	N444201TR16 40.70-41.70	N444201TR16 40.80	180527	3, 4, 5	25	40	10		15			10									28.1	1.49	26.6
Koivuniemi	N444201TR16 68.40-69.40	N444201TR16 69.20	180528	1	<1	40	15		20		Sillimanite (15)	4		Rutile	Sericite	1					0.3	<0.05	0.26
Koivuniemi	N444201TR16 89.00-91.00	N444201TR16 90.90	180529	4, 5	10	30	30		10	<1		15		Rutile	Sericite	3					8.45	<0.05	8.59
Koivuniemi	N444201TR17 36.55-38.55	N444201TR17 36.65	180530	3, 4	20	35	20		10	<1		10		Rutile	Sericite	2	Saussurite	2			15.5	0.19	15.3
Koivuniemi	N444201TR17 75.50-77.10	N444201TR17 76.70	180531	3, 4	10	40	10		15	1			25								8.65	<0.05	8.92
Koivuniemi	N444201TR18 32.30-34.30	N444201TR18 32.30	180532	1	3	30	15	20	30	1		2		Garnet	Sericite	1							
Koivuniemi	N444201TR18 94.80-96.10	N444201TR18 96.15	180533	5, (3)	25	30	25		10			10		Chalcopyrite	Sericite	3					15.8	0.53	15.3
Koivuniemi	N444201TR21 19.15-21.15	N444201TR21 20.80	180534	1, (4)	1	30	20	10	30		Garnet (3)	4		Zircon, Apatite	Sericite	1					0.82	<0.05	0.79
Koivuniemi	N444201TR21 43.65-45.65	N444201TR21 44.25	180535	1, (4)	1	25	25	15	20			9		Zircon, Chalcopyrite	Sericite	2	Saussurite	2			0.55	<0.05	0.51
Koivuniemi	N444201TR21 64.00-65.60	N444201TR21 64.75	180536	5, (3)	15	40	15		20			10			Sericite	1					12.8	0.1	12.7
Koivuniemi	N444201BR22 71.00-72.60	N444201BR22 71.50	180537	5, (3)	15	25	20		15	10		15									9.55	<0.05	9.54
Koivuniemi	N444201BR24 44.75-46.30	N444201BR24 44.75	180538	5, (3)	20	20	35		15			10		Zircon	Saussurite	2					12.8	<0.05	12.9
Saareke	N444201BR33 38.20-40.20	N444201BR33 39.40	180596	2	7	30	30		10	<1	Hornblende (10)	12		Chalcopyrite, Sphalerite	Sericite	1	Chlorite	2			4.47	0.07	4.4
Saareke	N444201BR34 52.80-54.70	N444201BR34 54.55	180597	2, (5)	5	30	25		10		Augite (10), Chlorite (5)	15		Chalcopyrite, Sphalerite	Sericite	2	Saussurite	2	Chlorite	1	1.69	0.12	1.58
Saareke	N444201BR34 69.80-71.70	N444201BR34 70.30	180598	2	6	30	25		5		Calcite/dolomite (5)	22		Chalcopyrite, Sphalerite	Sericite	2					4.47	0.49	3.98
Saareke	N444201BR35 37.00-38.70	N444201BR35 37.60	180599	2, (5)	5	25	25		15		Hornblende (10)	15		Chalcopyrite, Sphalerite	Sericite	2	Chlorite	1			2.54	0.21	2.33
Mineral modal amounts as % are visible estimations with microscope																							
Alteration intensity: 1- weak, 2 - moderate, 3 - strong																							

Appendix 2. EM-EDS – analysis data. Numbering after sample-id indicate spot analysis number.

Specimen	N4442017R16 40.80							N4442017R18 32.30						N4442018R24 44.75					N4442018R34 54.55			
Analyse number	1	2	3	4	5	6		1	2	3	4	5		1	2	3	4		1	2	3	4
C (wt %)	98.86	98.78	98.92	98.64	98.9	98.06		97.58	97.76	97.7	97.69	97.74		98.84	98.3	98.73	98.05		97.15	97.7	97.32	97.09
Na								0.1	0.11	0.11	0.09	0.12		0.07	0.12	0.17	0.16				0.14	
Mg								0.14	0.11	0.12	0.11	0.1		0.06	0.05				0.12	0.1		0.15
Al								0.47	0.46	0.47	0.47	0.46		0.28	0.47	0.36	0.57		0.35	0.38	0.5	0.53
Si	1.14	1.22	1.08	1.36	1.1	1.94		0.88	0.9	0.92	0.93	0.95		0.55	0.79	0.74	1.12		1.32	1.25	1.31	1.26
Fe								0.6	0.47	0.47	0.45	0.42		0.2	0.27				0.59	0.57	0.61	0.77
K								0.22	0.19	0.21	0.25	0.21					0.1				0.12	
F																			0.31			
Ca																			0.31			0.2